NATIONAL ADVISORY COMMITTEE FOR AERONAUTICS

TECHNICAL NOTE 3067

ROLLING EFFECTIVENESS AND AILERON REVERSAL OF RECTANGULAR WINGS AT SUPERSONIC SPEEDS

By John M. Hedgepeth and Robert J. Kell

Langley Aeronautical Laboratory
Langley Field, Va.

NACA

Washington
April 1954

1C

NATIONAL ADVISORY COMMITTEE FOR AERONAUTICS

TECHNICAL NOTE 3067

ROLLING EFFECTIVENESS AND AILERON REVERSAL OF RECTANGULAR WINGS AT SUPERSONIC SPEEDS

By John M. Hedgepeth and Robert J. Kell

SUMMARY

Linearized supersonic lifting-surface theory is used in conjunction with structural influence coefficients to formulate a method for analyzing the aeroelastic behavior in roll at supersonic speeds of a rectangular wing mounted on a cylindrical body. Rolling effectiveness and aileron-reversal speed are computed by using a numerical solution which incorporates matrices.

Results obtained for an example configuration by using this method are compared with the results obtained by using simplified methods of analysis. For the particular configuration considered, the variation of rolling effectiveness with Mach number is found for two constant-altitude flights.

INTRODUCTION

In the past, most aeroelastic calculations have been based on the use of beam theory for the structural analysis and strip theory for the aerodynamic analysis. The application of these simplified theories avoids complications which result from using more refined theories; in addition, the simplified theories are quite adequate, in most cases, when applied to wings of high aspect ratio. When applied to wings of low aspect ratio, however, these simple theories may become inadequate; if so, more refined structural and aerodynamic analyses are necessary.

The purpose of this paper is to describe a method for predicting aeroelastic effects on the steady-state roll of rectangular wings at supersonic speeds in those cases for which beam and strip theory are inadequate but for which the aerodynamic effects of chordwise deformation may be neglected. In this method the structural distortions caused by arbitrary loads are expressed in terms of structural influence functions. The aerodynamic loads caused by arbitrary angle-of-attack distributions are determined by superposing basic aerodynamic loadings resulting from unit-step angle-of-attack distributions, which loadings are obtained

herein on the basis of linearized aerodynamic theory. By means of this superposition procedure, first outlined by Frick and Chubb in reference 1, the application of three-dimensional lifting-surface theory is considerably simplified.

The aircraft configuration considered herein consists of two flexible rectangular wings with trailing-edge ailerons of constant chord, diametrically mounted on an infinitely long, rigid, cylindrical fuselage.

The analysis of the aeroelastic rolling behavior is separated into various parts. The analysis of the structural deformations is described, the aerodynamic loads are then found, and the two parts are combined. A numerical solution of the resulting equations is presented in matrix form. Tables of aerodynamic matrix elements usable for any rectangular plan form are included. A particular example is analyzed and the results are compared with those obtained by simplified methods. The structural analysis of the example configuration is included in appendix A and the details of the aerodynamic analysis are relegated to appendix B.

SYMBOLS

D	local flexural stiffness, $Et^3/12(1 - \mu^2)$
E	Young's modulus of elasticity
G	shear modulus of elasticity, $E/2(1 + \mu)$
$G_L(y,\eta)$	structural twist influence function which results from a unit concentrated load at the wing midchord
$G_M(y,\eta)$	structural twist influence function which results from a unit concentrated torque
$L(y)$	aerodynamic load per unit span, positive upward
M	free-stream Mach number
$M(y)$	aerodynamic moment, per unit span, about the midchord, positive in the positive twist direction
P_h	static pressure at altitude
P_0	standard static pressure at sea level
$Q(y)$	aerodynamic moment, per unit span, about the elastic axis, positive in the positive twist direction

V	free-stream velocity
a	ratio between fuselage radius and exposed wing semispan
b	total wing span, $2(al + l)$
b_a	single aileron span
c	wing chord
c_a	aileron chord
$e(y)$	distance measured forward from the midchord to the elastic axis, expressed as fraction of chord
l	exposed wing semispan
m	modified aspect-ratio parameter, $\beta l/c$
p	rolling angular velocity (see fig. 1)
$pb/2V$	tangent of the wing-tip helix angle
q	dynamic pressure
t	thickness of wing cross section
x,y,z	coordinate system (see fig. 1)
β	cotangent of the Mach angle, $\sqrt{M^2 - 1}$
$\beta c_l(y)$	section lift coefficient, $\frac{L(y)}{qc/\beta}$
$\beta c_m(y)$	section moment coefficient about the midchord, $\frac{M(y)}{qc^2/\beta}$
$\beta c_q(y)$	section moment coefficient about the elastic axis, $\frac{Q(y)}{qc^2/\beta}$
δ	aileron deflection (see fig. 1)
$\theta(y)$	angle of twist of wing (see fig. 1)
λ	structural parameter, $\frac{l}{c}\sqrt{24(1 - \mu)}$

μ	Poisson's ratio
$\sigma(x,y)$	local angle of attack of wing
ϕ	rolling effectiveness, $(pb/2V)_F/(pb/2V)_R$
$\varphi(x,y)$	velocity potential
$\Phi(x_1,y_1)$	nondimensionalized velocity potential

Subscripts:

F	flexible wing
R	rigid wing
a	airloads due to aileron deflection
r	airloads due to roll
s	airloads due to structural deformation
rev	aileron reversal
p	aerodynamic coefficients due to unit $pb/2V$
p_o	aerodynamic coefficients due to a unit rate of roll about the x-axis
α	aerodynamic coefficients due to a unit angle of attack of the entire wing
δ	aerodynamic coefficients due to a unit aileron deflection
θ	indicial aerodynamic coefficients due to a unit-step angle-of-attack distribution
I,II,...VI	regions on surface of wing
1	nondimensional quantities used in appendix B

Superscript:

'	aerodynamic coefficients due to a unit-step angle-of-attack distribution on one wing only

ANALYSIS

Structural Deformations

In this report the treatment of the structural deformations is based on the assumption that there is no chordwise bending of the wing. The effect of the structural distortion on the aerodynamic loads is then determined entirely by the angle of twist $\theta(y)$, the contribution of the spanwise bending being negligible. (See fig. 1.) Consequently, only the determination of $\theta(y)$ will be included in this analysis.

If the section lift $L(y)$ and the section moment about the midchord $M(y)$ are known, the angle of twist can be obtained from

$$\theta(y) = \int_0^l G_L(y,\eta)\ L(\eta)\ d\eta + \int_0^l G_M(y,\eta)\ M(\eta)\ d\eta \qquad (1)$$

In this equation, $G_L(y,\eta)$ and $G_M(y,\eta)$ are influence functions which define the twist at y caused by the application of a unit concentrated load at the midchord and a unit concentrated torque, respectively, at the station η. For many structures these influence functions may be obtained analytically as is done in appendix A for a uniform flat-plate wing; other structures may be handled analytically by methods such as those described in references 2, 3, and 4, for instance. For some structures, it may be more convenient or even necessary to resort to the use of experimental influence coefficients. The analysis proceeds hereinafter on the assumption that the influence functions are known.

In general, the two influence functions are needed in order to specify completely the twist of the wing. For many rectangular wings, however, sufficient accuracy can be obtained by expressing the twist solely in terms of the moment about some "elastic axis." This elastic axis is herein defined as a line along which loads can be placed without producing significant twist anywhere.

If an elastic axis does exist, it is no longer necessary to know the influence function associated with load; only $G_M(y,\eta)$ need be determined. The twist, in this case, is given by

$$\theta(y) = \int_0^l G_M(y,\eta)\ Q(\eta)\ d\eta \qquad (2)$$

In this equation, $Q(y)$ is the section torque about the elastic axis and can be expressed in terms of $L(y)$ and $M(y)$ by means of the simple moment-transfer relation

$$Q(y) = M(y) - e(y)\ c\ L(y) \tag{3}$$

where $e(y)$ is the distance measured forward from the midchord to the elastic axis, expressed as a fraction of the chord.

Aerodynamic Loads

The section lift $L(y)$ and moment $M(y)$ may be expressed in coefficient form as

$$\left.\begin{aligned} L(y) &= \frac{qc}{\beta}\,\beta c_l(y) \\ M(y) &= \frac{qc^2}{\beta}\,\beta c_m(y) \end{aligned}\right\} \tag{4}$$

For convenience, the products of $\beta = \sqrt{M^2 - 1}$ and the coefficients are considered herein rather than the coefficients themselves.

It is assumed that the aircraft is undergoing a steady roll about the axis of the body and that this axis is in line with the direction of flight. Consequently, the resulting loads are due solely to structural twist of the wing, the rolling velocity itself, and the deflection of the ailerons. Since linear aerodynamic theory is to be used, the coefficients resulting from this steady rolling maneuver can be expressed as

$$\left.\begin{aligned} \beta c_l &= (\beta c_l)_s + (\beta c_l)_r + (\beta c_l)_a \\ \beta c_m &= (\beta c_m)_s + (\beta c_m)_r + (\beta c_m)_a \end{aligned}\right\} \tag{5}$$

where s, r, and a refer, respectively, to structural deformation, roll, and aileron deflection.

In the determination of the coefficients on the right-hand side of equations (5) the wing and body must be treated as a unit. In view of the fact that in this problem the pressures resulting from the presence of the body are important only in the neighborhood of the wing root and therefore contribute only slightly to the structural distortions and

rolling moment, a rather simple idealization is made regarding the body; that is, the body is replaced by a rigid plate joining the two wing roots together. The width of this plate is the same as the body diameter. (See fig. 2(a).) While it is not argued that this idealization is the most nearly correct one, the resulting aeroelastic model does have the advantage of simplicity and allows aerodynamic interaction between the two wings. The presence of the cylindrical body is further taken into account by neglecting the effects upon the rolling moment of the pressures acting on the rigid plate, since the pressures acting on the actual cylindrical body would produce no rolling moment.

Although the details of the calculations of the aerodynamic loads have been relegated to appendix B, a short discussion of the loads due to each of the three causes - structural deformation, roll, and aileron deflection - is included in the subsequent portions of this section.

Loads due to structural deformation.- As a consequence of the previously assumed linearity of chordwise deformation, the local angle of attack of the wing is completely defined by the twist of the wing. Since the twist is not defined explicitly, the deformations being dependent on loads which are, in turn, dependent on the twist itself, it is necessary to be able to perform the rather difficult task of calculating the aerodynamic loads caused by an arbitrary angle-of-attack distribution. This task is considerably simplified for the rolling problem by superposing loads caused by an antisymmetrical unit-step angle-of-attack distribution obtained by imposing a positive unit angle of attack outboard of any spanwise station η on the right wing and a negative unit angle of attack over the corresponding portion of the left wing as shown in figure 2(b). These basic load distributions, which have the nature of aerodynamic influence functions, are hereinafter called "indicial" loads for the sake of brevity. Superposition of the indicial section coefficients of lift and twisting moment, designated $\beta c_{l_\theta}(y,\eta)$ and $\beta c_{m_\theta}(y,\eta)$, respectively, which result from such basic angle-of-attack distributions, yields the section coefficients $\left[\beta c_l(y)\right]_s$ and $\left[\beta c_m(y)\right]_s$ due to structural deformation. The required superposition integrals are given by

$$\left.\begin{aligned} \left[\beta c_l(y)\right]_s &= \int_0^l \beta c_{l_\theta}(y,\eta)\,\frac{d\theta}{d\eta}\,d\eta \\ \left[\beta c_m(y)\right]_s &= \int_0^l \beta c_{m_\theta}(y,\eta)\,\frac{d\theta}{d\eta}\,d\eta \end{aligned}\right\} \tag{6}$$

where the twist at the root is assumed to be zero.

The indicial section coefficients are dependent not only on the spanwise coordinate y and the position of the step η but also on two additional parameters. These parameters are the modified aspect-ratio parameter $\beta l/c$, which usually appears in theoretical supersonic aerodynamic calculations, and the nondimensional body radius a. The dependency on the body radius is undesirable since it restricts the application of these indicial section coefficients to a particular value of a. Fortunately the dependency can be eliminated by making use of the fact that the loads due to the antisymmetrical unit-step angle-of-attack distribution can be separated into two parts: the first is the loads due to a unit-step angle of attack on the right wing only (see fig. 2(c)); the second is the loads due to a negative unit-step angle of attack on the left wing only. It can be seen that the second part is merely the negative mirror image of the first and, consequently, only the first case need be considered in detail. The total indicial section coefficients can be written in terms of these partial indicial section coefficients, designated $\beta c_{l_\theta}'$ and $\beta c_{m_\theta}'$, as follows:

$$\left.\begin{aligned} \beta c_{l_\theta}(y,\eta) &= \beta c_{l_\theta}'(y,\eta) - \beta c_{l_\theta}'(-2al-y,\eta) \\ \beta c_{m_\theta}(y,\eta) &= \beta c_{m_\theta}'(y,\eta) - \beta c_{m_\theta}'(-2al-y,\eta) \end{aligned}\right\} \tag{7}$$

The first term on the right-hand side in equations (7) gives the contribution of the right-hand step angle of attack; the second term gives the contribution of the negative left-hand step.

The advantage of the foregoing separation is that $\beta c_{l_\theta}'$ and $\beta c_{m_\theta}'$ are independent of the body radius and are functions of only the modified aspect-ratio parameter, provided that this parameter is greater than $\frac{1}{1+2a}$, that is, when the Mach number is great enough so that there is no point on either wing that is influenced by both wing tips simultaneously. Thus, if the restriction $\frac{\beta l}{c} > \frac{1}{1+2a}$ is imposed, a single parameter remains - $\beta l/c$ itself - and it is feasible to compute tables applicable for any body radius. Numerical values of $\beta c_{l_\theta}'$ and $\beta c_{m_\theta}'$ for $-\frac{c}{\beta l} \leqq \frac{y}{l} \leqq 1$ and $0 \leqq \frac{\eta}{l} \leqq 1$ in steps of 0.1 are presented in table I for several values of $\beta l/c$. These numerical values were obtained from expressions derived in appendix B.

Loads due to roll.- The section loading coefficients resulting from roll can be written in the form

$$\left.\begin{aligned}\left(\beta c_l\right)_r &= \beta c_{l_p} \frac{pb}{2V} \\ \left(\beta c_m\right)_r &= \beta c_{m_p} \frac{pb}{2V}\end{aligned}\right\} \tag{8}$$

The rolling derivatives βc_{l_p} and βc_{m_p} are given in appendix B. Here again the derivatives are dependent on both $\beta l/c$ and a. Inspection of the resulting expressions (eqs. (B13) and (B14)), however, reveals that the dependence on a is quite simple; the expressions for βc_{l_p} and βc_{m_p} can each be separated into two parts - one with the coefficient $\frac{a}{1+a}$, the other with $\frac{1}{1+a}$ - both of which parts are independent of a. It is possible to show that in each case the first part is merely the derivative which results from a unit angle of attack of the entire wing and the second part is the rolling derivative which would result if the wing were rolling about the x-axis. Therefore, these expressions become

$$\left.\begin{aligned}\beta c_{l_p} &= -\frac{a}{1+a} \beta c_{l_\alpha} + \frac{1}{1+a} \beta c_{l_{p_o}} \\ \beta c_{m_p} &= -\frac{a}{1+a} \beta c_{m_\alpha} + \frac{1}{1+a} \beta c_{m_{p_o}}\end{aligned}\right\} \tag{9}$$

In order for this simplification to be correct, it is again necessary to impose the restriction $\frac{\beta l}{c} > \frac{1}{1+2a}$.

The quantities βc_{l_α}, βc_{m_α}, $\beta c_{l_{p_o}}$, and $\beta c_{m_{p_o}}$ have been calculated for values of $0 \leqq \frac{y}{l} \leqq 1$ in steps of 0.1 and are presented in table II for several values of $\beta l/c$.

Loads due to aileron deflection.- The section coefficients of lift and twisting moment,

$$\left.\begin{aligned} \left(\beta c_l\right)_a &= \beta c_{l_\delta} \delta \\ \left(\beta c_m\right)_a &= \beta c_{m_\delta} \delta \end{aligned}\right\} \quad \text{and} \qquad (10)$$

respectively, are found for constant-chord trailing-edge ailerons of arbitrary length. All gaps between the wing and aileron are considered to be sealed. The calculation of the aileron derivatives βc_{l_δ} and βc_{m_δ} is very similar to that of the indicial structural loads and is included in appendix B. For most reasonable aileron configurations, if the aircraft is flying at supersonic speeds sufficiently high to satisfy the Mach number limitation previously imposed $\left(\text{that is, } \frac{\beta l}{c} > \frac{1}{1 + 2a}\right)$, an aileron deflection on the left wing produces no loads on the right wing. For this reason, only the case is considered wherein the loads on one wing are independent of the aileron deflection on the other. In this case, the limitation on the modified aspect-ratio parameter $\beta l/c$ for the analysis of aileron loadings in appendix B is that $\beta l/c$ must be greater than $\frac{c_a/c}{1 + 2a - \frac{b_a}{l}}$. Numerical values are given in table III for $0 \leqq \frac{y}{l} \leqq 1$ in intervals of 0.1 for several values of $\beta l/c$; the computations have been made for $b_a/l = 1.0$ and $c_a/c = 0.2$.

Significance of Mach number limitations.- Although the restrictions that have been placed upon the modified aspect-ratio parameter limit the utility of the aerodynamic results contained herein, these restrictions, in reality, are not serious. This fact is substantiated by considering a typical configuration such as that used for the example contained in a subsequent section. For this wing, which has an aspect ratio of 3.6, the pertinent parameters are $l/c = 1.5$, $a = 0.2$, $c_a/c = 0.2$, and $b_a/l = 1$. The restriction imposed upon the expressions for the loads due to structural deformation and roll, $\frac{\beta l}{c} > \frac{1}{1 + 2a}$, and that for the loads caused by aileron deflection, $\frac{\beta l}{c} > \frac{c_a/c}{1 + 2a - \frac{b_a}{l}}$, become $M > 1.108$ and $M > 1.054$, respectively. Since the validity of linear aerodynamic

theory is questionable near a Mach number of 1, these limitations are of little consequence.

Aeroelastic Solution

Structural and rolling-moment equations.- In the solution of the aeroelastic rolling problem, not only must structural equilibrium (eq. (1)) be satisfied but also the equilibrium of moments about the rolling axis. If the loads in equation (1) are replaced by the loads arising from the various causes as derived in the preceding section, the equation specifying structural equilibrium becomes

$$\theta(y) = \frac{qc}{\beta}\int_0^l \left[G_L(y,\eta) \int_0^l \beta c_{l_\theta}(\eta,\zeta)\, \frac{d\theta}{d\zeta}\, d\zeta + c\, G_M(y,\eta) \int_0^l \beta c_{m_\theta}(\eta,\zeta)\, \frac{d\theta}{d\zeta}\, d\zeta \right] d\eta + \frac{qc}{\beta}\frac{pb}{2V}\int_0^l \left[G_L(y,\eta)\, \beta c_{l_p}(\eta) + c\, G_M(y,\eta)\, \beta c_{m_p}(\eta) \right] d\eta + \frac{qc}{\beta}\delta \int_0^l \left[G_L(y,\eta)\, \beta c_{l_\delta}(\eta) + c\, G_M(y,\eta)\, \beta c_{m_\delta}(\eta) \right] d\eta \qquad (11)$$

Rolling-moment equilibrium is attained by setting the total rolling moment equal to zero. This condition can be written as

$$\int_0^l (al + \eta)\, L(\eta)\, d\eta = 0$$

Again, the results of the preceding section can be used to give

$$\frac{qc}{\beta}\int_0^l (al + \eta)\left[\int_0^l \beta c_{l_\theta}(\eta,\zeta)\, \frac{d\theta}{d\zeta}\, d\zeta + \frac{pb}{2V}\, \beta c_{l_p}(\eta) + \delta\, \beta c_{l_\delta}(\eta) \right] d\eta = 0 \qquad (12)$$

Alternate structural equation.- Equations (11) and (12) completely express the necessary conditions for this aeroelastic problem. It is to be noted that the quantities δ and qc/β are, in general, known, the structural twist $\theta(y)$ is unknown, and the aeroelastic rolling rate $pb/2V$ is the quantity that is desired. The simultaneous solution of these equations in closed form is, in actuality, extremely difficult if not impossible to obtain. Some sort of numerical solution is therefore inevitable. One type of numerical solution, which utilizes a collocation technique in the solution of equations (11) and (12), is derived in a subsequent section.

The numerical methods with which the indicated integrations in equations (11) and (12) are performed can be expected to be accurate when applied to reasonably well-behaved functions. In addition to numerical integration, however, numerical differentiation must be used in order to express the rate of twist $d\theta/dy$, upon which the loads due to structural deformation depend, in terms of the twist θ. As is well known, the process of numerical differentiation is not as accurate as that of numerical integration and therefore should be avoided if possible. The numerical differentiation can be eliminated by differentiating equation (11) with respect to y, which operation yields

$$\frac{d\theta}{dy} = \frac{qc}{\beta}\int_0^l \left[\frac{\partial G_L(y,\eta)}{\partial y}\int_0^l \beta c_{l_\theta}(\eta,\zeta)\,\frac{d\theta}{d\zeta}\,d\zeta + c\,\frac{\partial G_M(y,\eta)}{\partial y}\int_0^l \beta c_{m_\theta}(\eta,\zeta)\,\frac{d\theta}{d\zeta}\,d\zeta\right]d\eta + \frac{qc}{\beta}\frac{pb}{2V}\int_0^l \left[\frac{\partial G_L(y,\eta)}{\partial y}\,\beta c_{l_p}(\eta) + c\,\frac{\partial G_M(y,\eta)}{\partial y}\,\beta c_{m_p}(\eta)\right]d\eta + \frac{qc}{\beta}\delta\int_0^l \left[\frac{\partial G_L(y,\eta)}{\partial y}\,\beta c_{l_\delta}(\eta) + c\,\frac{\partial G_M(y,\eta)}{\partial y}\,\beta c_{m_\delta}(\eta)\right]d\eta \qquad (13)$$

In this manner, equilibrium equation (11) is replaced by equation (13) and the twist θ no longer appears in the problem. The rate of twist becomes the unknown and can be used directly in the numerical solution.

The use of equations (12) and (13) is particularly desirable when the functions $\frac{\partial G_L(y,\eta)}{\partial y}$ and $\frac{\partial G_M(y,\eta)}{\partial y}$, which are merely the rates of

twist due to concentrated loads and torques, respectively, can be found accurately. The example considered in a subsequent section is one for which it was possible to obtain these functions analytically. When complicated structures are to be dealt with, however, recourse must usually be made to experiment or to approximate theories in obtaining the structural properties. For these structures, probably only discrete influence coefficients for twist can be found; the determination of the rate-of-twist influence functions would be subject to at least the same inherent inaccuracies as the numerical differentiation discussed previously. In such cases, therefore, the use of equation (13) instead of equation (11) would not be advantageous.

Aileron reversal.- If the rolling-moment equation (12) is solved for δ, the result is substituted into equation (11) or equation (13), and $pb/2V$ is set equal to zero, the following equations result:

For equation (11),

$$\theta(y) = \frac{q_{rev}c}{\beta}\left\{\int_0^l \left[G_L(y,\eta)\int_0^l \beta c_{l_\theta}(\eta,\zeta)\,\frac{d\theta}{d\zeta}\,d\zeta + c\,G_M(y,\eta)\int_0^l \beta c_{m_\theta}(\eta,\zeta)\,\frac{d\theta}{d\zeta}\,d\zeta\right]d\eta - \frac{\int_0^l \left[G_L(y,\eta)\,\beta c_{l_\delta}(\eta) + c\,G_M(y,\eta)\,\beta c_{m_\delta}(\eta)\right]d\eta}{\int_0^l (al+\eta)\,\beta c_{l_\delta}(\eta)\,d\eta} \times \int_0^l (al+\eta)\int_0^l \beta c_{l_\theta}(\eta,\zeta)\,\frac{d\theta}{d\zeta}\,d\zeta\,d\eta\right\} \tag{14}$$

For equation (13),

$$\frac{d\theta(y)}{dy} = \frac{q_{rev}c}{\beta}\left\{\int_0^l\left[\frac{\partial G_L(y,\eta)}{\partial y}\int_0^l \beta c_{l_\theta}(\eta,\zeta)\,\frac{d\theta}{d\zeta}\,d\zeta + c\,\frac{\partial G_M(y,\eta)}{\partial y}\int_0^l \beta c_{m_\theta}(\eta,\zeta)\,\frac{d\theta}{d\zeta}\,d\zeta\right]d\eta - \frac{\int_0^l\left[\frac{\partial G_L(y,\eta)}{\partial y}\,\beta c_{l_\delta}(\eta) + c\,\frac{\partial G_M(y,\eta)}{\partial y}\,\beta c_{m_\delta}(\eta)\right]d\eta}{\int_0^l (a\iota + \eta)\,\beta c_{l_\delta}(\eta)\,d\eta}\times \int_0^l (a\iota + \eta)\int_0^l \beta c_{l_\theta}(\eta,\zeta)\,\frac{d\theta}{d\zeta}\,d\eta\right\} \tag{15}$$

Either of these homogeneous integral equations expresses the condition for aileron reversal, where the dynamic pressure at reversal q_{rev} appears as an eigenvalue.

Rolling effectiveness.- The effect of the elasticity of the wing on the rolling behavior may be determined by examining the ratio between the rate of roll of the flexible wing and the rate of roll which would occur if the wing were rigid. This ratio, the "rolling effectiveness," is designated as ϕ, where

$$\phi = \frac{(pb/2V)_F}{(pb/2V)_R}$$

In this equation $(pb/2V)_F$ is the rate of roll determined directly from the aeroelastic equations. The quantity $(pb/2V)_R$, the rate of roll

for the rigid wing, is found by setting the twist per unit length equal to zero in equation (12):

$$\left(\frac{pb}{2V}\right)_R = -\delta \frac{\int_0^l (al + y)\ \beta c_{l_\delta}(y)\ dy}{\int_0^l (al + y)\ \beta c_{l_p}(y)\ dy} \tag{16}$$

Simplifications for wings with an elastic axis.- If the wing is constructed in such a manner that an elastic axis does exist as previously described, the expression for structural equilibrium is given by equation (2) instead of equation (1). It is to be remembered that, in this case, the twists are dependent only on $Q(y)$, the torque about the elastic axis, and not on the load $L(y)$. The aeroelastic structural-equilibrium equation which results from using equation (2) instead of equation (1) can be obtained by merely deleting the terms in equation (11) that involve $G_L(y,\eta)$ and replacing the section moment coefficients about the midchord by the section moment coefficients about the elastic axis. Thus, the derivatives βc_{m_θ}, βc_{m_p}, and βc_{m_δ} should be replaced by βc_{q_θ}, βc_{q_p}, and βc_{q_δ}, respectively, where

$$\left.\begin{aligned} \beta c_{q_\theta} &= \beta c_{m_\theta} - e\ \beta c_{l_\theta} \\ \beta c_{q_p} &= \beta c_{m_p} - e\ \beta c_{l_p} \\ \beta c_{q_\delta} &= \beta c_{m_\delta} - e\ \beta c_{l_\delta} \end{aligned}\right\} \tag{17}$$

In these equations, as before, e is the distance measured forward from the midchord to the elastic axis, expressed as a fraction of the chord.

The equations analogous to equations (13), (14), and (15) are obtained in exactly the same manner.

NUMERICAL METHOD

Since an exact solution of the aeroelastic equations is not feasible, even for the simplest configuration, this section is devoted to the

presentation of a numerical method of solution. The method is based on satisfying the equations at a number of discrete spanwise stations. Matrix notation is used as an aid in organizing the numerical procedure. A step-by-step outline of the procedure is included at the end of this section in order to aid the reader.

The accuracy of the numerical method is directly dependent upon the number of stations used. Experience has shown that for this particular problem 11 stations, defined by the end points of 10 equal spanwise intervals, are sufficient. The derivation that follows is therefore based on 10 equal intervals, the extension to other numbers of intervals being evident. Simpson's rule is used to perform the integrations and parabolic difference equivalents are used to replace any necessary derivatives.

Matrix Operations

Two distinct types of integration appear in the aeroelastic equation. The first is of the form

$$\int_0^l f(\eta)\, g(\eta)\, d\eta$$

and the second is of the form

$$\int_0^l h(y,\eta)\, g(\eta)\, d\eta$$

The integrands in these equations are evaluated at each of the spanwise stations $\eta_0, \eta_1, \eta_2, \ldots \eta_i, \ldots \eta_{10}$, where, for equal intervals of width ϵ, $\eta_i = i\epsilon$. In a similar manner this subscript notation is used to denote evaluation of the integrands at each spanwise station. Thus, $f_i = f(\eta_i) = f(i\epsilon)$, $g_i = g(\eta_i) = g(i\epsilon)$, and $h_{ij} = h(y_i,\eta_j) = h(i\epsilon,j\epsilon)$. For 10 intervals, $\epsilon = l/10$ and Simpson's rule becomes, for each of the integrals, respectively,

$$\int_0^l f(\eta)\, g(\eta)\, d\eta = \frac{l}{30}\left(f_0g_0 + 4f_1g_1 + 2f_2g_2 + 4f_3g_3 + \ldots + 4f_9g_9 + f_{10}g_{10}\right)$$

and (for any single y_i)

$$\int_0^l h(y_i,\eta)\, g(\eta)\, d\eta = \frac{l}{30}\left(h_{i0}g_0 + 4h_{i1}g_1 + 2h_{i2}g_2 + 4h_{i3}g_3 + \cdots + 4h_{i9}g_9 + h_{i,10}g_{10}\right)$$

In matrix form these integrals can be written as, respectively,

$$\int_0^l f(\eta)\, g(\eta)\, d\eta = \left\lfloor f_i \right\rfloor \left[S \right] \left| g_i \right|$$

and (for all y_i)

$$\left| \left(\int_0^l h(y,\eta)\, g(\eta)\, d\eta \right)_i \right| = \left[h_{ij} \right] \left[S \right] \left| g_j \right|$$

The row matrix is given by

$$\left\lfloor f_i \right\rfloor = \left\lfloor f_0\ f_1\ f_2\ f_3 \cdots f_9\ f_{10} \right\rfloor$$

and a typical column matrix by

$$\left| g_i \right| = \begin{vmatrix} g_1 \\ g_2 \\ g_3 \\ \cdot \\ \cdot \\ \cdot \\ g_9 \\ g_{10} \end{vmatrix}$$

where the subscripts denote the position of each element. The square matrix is given by

$$\left[h_{ij}\right] = \begin{bmatrix} h_{00} & h_{01} & h_{02} & \cdots & h_{0,10} \\ h_{10} & h_{11} & h_{12} & \cdots & h_{1,10} \\ h_{20} & h_{21} & h_{22} & \cdots & h_{2,10} \\ \cdot & \cdot & \cdot & \cdots & \cdot \\ h_{10,0} & h_{10,1} & h_{10,2} & \cdots & h_{10,10} \end{bmatrix}$$

where the first subscript designates the row and the second subscript designates the column in which an element appears. This subscript notation is used throughout this section. The integrating matrix is given by

$$\left[S\right] = \frac{l}{30}\begin{bmatrix} 1 & & & & & & & & & \\ & 4 & & & & & & & & \\ & & 2 & & & & & & & \\ & & & 4 & & & & & & \\ & & & & 2 & & & & & \\ & & & & & 4 & & & & \\ & & & & & & 2 & & & \\ & & & & & & & 4 & & \\ & & & & & & & & 2 & \\ & & & & & & & & & 1 \end{bmatrix} \tag{18}$$

All derivatives which appear in the aeroelastic equation are of first order; difference equivalents based on passing a parabola through three adjacent points are used herein to approximate the derivatives. For the points $i = 1, 2, \ldots 9$ the standard difference equivalent derived by finding the slope at the center of the three ordinates is used:

$$\left(\frac{df}{dy}\right)_i = \frac{f_{i+1} - f_{i-1}}{2\epsilon}$$

For the end points $i = 0$ and $i = 10$, the slope at the exterior of the three ordinates must be used:

$$\left(\frac{df}{dy}\right)_0 = \frac{-3f_0 + 4f_1 - f_2}{2\epsilon}$$

$$\left(\frac{df}{dy}\right)_{10} = \frac{f_8 - 4f_9 + 3f_{10}}{2\epsilon}$$

In matrix form with $\epsilon = l/10$, these expressions become

$$\left|\left(\frac{df}{dy}\right)_i\right| = \left[D\right]\left|f_i\right|$$

where the differentiating matrix

$$\left[D\right] = \frac{5}{l}\begin{bmatrix} -3 & 4 & -1 & & & & & & & \\ -1 & 0 & 1 & & & & & & & \\ & -1 & 0 & 1 & & & & & & \\ & & -1 & 0 & 1 & & & & & \\ & & & -1 & 0 & 1 & & & & \\ & & & & -1 & 0 & 1 & & & \\ & & & & & -1 & 0 & 1 & & \\ & & & & & & -1 & 0 & 1 & \\ & & & & & & & -1 & 0 & 1 \\ & & & & & & & & 1 & -4 & 3 \end{bmatrix} \tag{19}$$

Aeroelastic Matrix Equation

The aeroelastic equations may now be written in matrix form by using the results of the foregoing numerical analysis of integrating

and differentiating processes. Equations (11) and (12) become, respectively,

$$\left|\theta_i\right| = \frac{qc}{\beta}\left\{\left[\left(G_L\right)_{ij}\right]\left[\ S\ \right]\left[\left(\beta c_{l_\theta}\right)_{jk}\right]\left[\ S\ \right]\left[\ D\ \right]\left|\theta_k\right| + c\left[\left(G_M\right)_{ij}\right]\left[\ S\ \right]\left[\left(\beta c_{m_\theta}\right)_{jk}\right]\left[\ S\ \right]\left[\ D\ \right]\left|\theta_k\right|\right\} + \frac{qc}{\beta}\frac{pb}{2V}\left\{\left[\left(G_L\right)_{ij}\right]\left[\ S\ \right]\left|\left(\beta c_{l_p}\right)_j\right| + c\left[\left(G_M\right)_{ij}\right]\left[\ S\ \right]\left|\left(\beta c_{m_p}\right)_j\right|\right\} + \frac{qc}{\beta}\delta\left\{\left[\left(G_L\right)_{ij}\right]\left[\ S\ \right]\left|\left(\beta c_{l_\delta}\right)_j\right| + c\left[\left(G_M\right)_{ij}\right]\left[\ S\ \right]\left|\left(\beta c_{m_\delta}\right)_j\right|\right\} \tag{20}$$

and

$$\frac{qc}{\beta}\left\{\left|al + y_j\right|\left[\ S\ \right]\left[\left(\beta c_{l_\theta}\right)_{jk}\right]\left[\ S\ \right]\left[\ D\ \right]\left|\theta_k\right| + \frac{pb}{2V}\left|al + y_j\right|\left[\ S\ \right]\left|\left(\beta c_{l_p}\right)_j\right| + \delta\left|al + y_j\right|\left[\ S\ \right]\left|\left(\beta c_{l_\delta}\right)_j\right|\right\} = 0 \tag{21}$$

If these equations are divided through by δ and the resulting matrix equations are combined, the following partitioned matrix equation results:

$$\left[\begin{array}{c|c} \dfrac{1}{\frac{qc}{\beta}}\left[I\right] - \left[A_{ik}\right] & \left|B_i\right| \\ \hline \left\lfloor D_k \right\rfloor & E \end{array}\right] \left|\begin{array}{c} \left|\theta_k/\delta\right| \\ \hline \left|\frac{pb}{2V}/\delta\right| \end{array}\right| = \left|\begin{array}{c} \left|C_i\right| \\ \hline F \end{array}\right| \tag{22}$$

where $\left[I\right]$ is the unit matrix. The submatrices are given by

$$\left[A_{ik}\right] = \left[\left(G_L\right)_{ij}\right]\left[S\right]\left[\left(\beta c_{l_\theta}\right)_{jk}\right]\left[S\right]\left[D\right] + c\left[\left(G_M\right)_{ij}\right]\left[S\right]\left[\left(\beta c_{m_\theta}\right)_{jk}\right]\left[S\right]\left[D\right]$$

$$\left|B_i\right| = -\left[\left(G_L\right)_{ij}\right]\left[S\right]\left|\left(\beta c_{l_p}\right)_j\right| - c\left[\left(G_M\right)_{ij}\right]\left[S\right]\left|\left(\beta c_{m_p}\right)_j\right|$$

$$\left|C_i\right| = \left[\left(G_L\right)_{ij}\right]\left[S\right]\left|\left(\beta c_{l_\delta}\right)_j\right| + c\left[\left(G_M\right)_{ij}\right]\left[S\right]\left|\left(\beta c_{m_\delta}\right)_j\right|$$

$$\left\lfloor D_k \right\rfloor = -\left\lfloor a_l + y_j \right\rfloor\left[S\right]\left[\left(\beta c_{l_\theta}\right)_{jk}\right]\left[S\right]\left[D\right]$$

$$E = -\left[a_l + y_j\right]\left[\quad S \quad\right]\left|\left(\beta c_{l_p}\right)_j\right|$$

$$F = \left[a_l + y_j\right]\left[\quad S \quad\right]\left|\left(\beta c_{l_\delta}\right)_j\right|$$

where

$$i, j, k = 0, 1, 2, \ldots 10$$

For a given configuration flying at a given speed and altitude, all the quantities in equation (22) are known except the twist θ at each station and the rate of roll $\frac{pb}{2V}/\delta$; solution of this matrix equation yields these quantities.

The rigid rate of roll, as found by expressing the integrals in equation (16) in numerical form, is merely

$$\left(\frac{pb}{2V}/\delta\right)_R = \frac{F}{E} \tag{23}$$

If the rate-of-twist influence coefficients are known, it is preferable to employ equation (13) instead of equation (11). In this case, the partitioned matrix equation analogous to equation (22) is

$$\left[\begin{array}{c|c} \frac{1}{\frac{qc}{\beta}}\left[I\right] - \left[\overline{A_{ik}}\right] & \left|\overline{B_i}\right| \\ \hline \left[\overline{D_k}\right] & E \end{array}\right] \left|\begin{array}{c} \left|\frac{\left(\frac{d\theta}{dy}\right)_k}{\delta}\right| \\ \hline \frac{pb}{2V}/\delta \end{array}\right| = \left|\begin{array}{c} \left|\overline{C_i}\right| \\ \hline F \end{array}\right| \tag{24}$$

where the submatrices are given by

$$\left[\overline{A_{ik}}\right] = \left[\left(\frac{\partial G_L}{\partial y}\right)_{ij}\right]\left[S\right]\left[\left(\beta c_{l_\theta}\right)_{jk}\right]\left[S\right] + c\left[\left(\frac{\partial G_M}{\partial y}\right)_{ij}\right]\left[S\right]\left[\left(\beta c_{m_\theta}\right)_{jk}\right]\left[S\right]$$

$$\left|\overline{B_i}\right| = -\left[\left(\frac{\partial G_L}{\partial y}\right)_{ij}\right]\left[S\right]\left|\left(\beta c_{l_p}\right)_j\right| - c\left[\left(\frac{\partial G_M}{\partial y}\right)_{ij}\right]\left[S\right]\left|\left(\beta c_{m_p}\right)_j\right|$$

$$\left|\overline{C_i}\right| = \left[\left(\frac{\partial G_L}{\partial y}\right)_{ij}\right]\left[S\right]\left|\left(\beta c_{l_\delta}\right)_j\right| + c\left[\left(\frac{\partial G_M}{\partial y}\right)_{ij}\right]\left[S\right]\left|\left(\beta c_{m_\delta}\right)_j\right|$$

$$\left[\overline{D_k}\right] = -\left[al + y_j\right]\left[S\right]\left[\left(\beta c_{l_\theta}\right)_{jk}\right]\left[S\right]$$

and the expressions for the scalars E and F remain the same as those given immediately after equation (22).

By applying the same numerical processes, the aileron-reversal equation (14) (or eq. (15)) can be put in matrix form. Equation (14), in which θ is the variable, becomes

$$\left|\theta_i\right| = \frac{q_{rev}c}{\beta}\left[\left[A_{ik}\right] + \left|C_i\right|\frac{1}{F}\left[D_k\right]\right]\left|\theta_k\right| \qquad (25)$$

The submatrices are defined immediately after equation (22).

Similarly, equation (15), where $d\theta/dy$ is the variable, becomes

$$\left|\left(\frac{d\theta}{dy}\right)_i\right| = \frac{q_{rev}c}{\beta}\left[\left[\overline{A_{ik}}\right] + \left|\overline{C_i}\right|\left|\frac{1}{F}\right|\left[\overline{D_k}\right]\right]\left|\left(\frac{d\theta}{dy}\right)_k\right| \tag{26}$$

The submatrices are defined immediately after equation (24).

A solution to equation (25) (or eq. (26)) is easily found by using matrix iteration. The process converges to give the lowest eigenvalue from which the dynamic pressure at aileron reversal may be obtained.

Reduced Matrix Equations

Up to this point, the numerical analysis has been based on the use of 11 spanwise stations, a number that was deemed necessary in order to obtain the desired accuracy because of the ill-behaved nature of some of the aerodynamic loading functions. In most cases, however, the twist (or rate of twist) is well behaved and, therefore, requires fewer stations for adequate specification. Utilization of this fact allows a considerable saving in the amount of work necessary to solve the matrix equations because of the fewer degrees of freedom involved.

If either the twist or the rate of twist is specified at the even-numbered stations, an interpolation procedure can be used to determine the values at all 11 stations. The particular type of interpolation used herein is obtained by passing a fifth-degree polynomial through the even-numbered stations and then evaluating this polynomial at the odd-numbered stations. This interpolating procedure can be written in matrix form as

$$\left|\theta_k\right| = \left[T_{kl}\right]\left|\theta_l\right|$$

or

$$\left|\left(\frac{d\theta}{dy}\right)_k\right| = \left[T_{kl}\right]\left|\left(\frac{d\theta}{dy}\right)_l\right|$$

where $k = 0, 1, 2, \ldots 10$ and $l = 0, 2, 4, \ldots 10$ and the interpolating matrix $\left[T_{kl}\right]$ is given by

$$\left[T_{kl}\right] = \begin{bmatrix} 1 & 0 & 0 & 0 & 0 & 0 \\ 0.246094 & 1.230468 & -0.820312 & 0.492187 & -0.175781 & 0.027344 \\ 0 & 1 & 0 & 0 & 0 & 0 \\ -0.027344 & 0.410156 & 0.820312 & -0.273437 & 0.082031 & -0.011718 \\ 0 & 0 & 1 & 0 & 0 & 0 \\ 0.011718 & -0.097656 & 0.585938 & 0.585938 & -0.097656 & 0.011718 \\ 0 & 0 & 0 & 1 & 0 & 0 \\ -0.011718 & 0.082031 & -0.273437 & 0.820312 & 0.410156 & -0.027344 \\ 0 & 0 & 0 & 0 & 1 & 0 \\ 0.027344 & -0.175781 & 0.492187 & -0.820312 & 1.230468 & 0.246094 \\ 0 & 0 & 0 & 0 & 0 & 1 \end{bmatrix} \tag{27}$$

The twist (or rate of twist) now needs to be known only at the even-numbered stations, the quantities at the odd-numbered stations being obtained by interpolation. Therefore, only the even rows of the influence-function matrices are necessary; these matrices become rectangular with 11 columns and 6 rows. When these simplifications are used to write the matrix equations for equations (11) and (12) and the resulting equations are combined, the following partitioned matrix equation results:

$$\left[\begin{array}{c|c} \frac{1}{\frac{qc}{\beta}}\left[\ I\ \right] - \left[A_{ml}^{*}\right] & \left|B_m^{*}\right| \\ \hline \left[\ D_l^{*}\ \right] & E \end{array}\right] \left|\begin{array}{c} \left|\theta_l/\delta\right| \\ \hline \frac{pb}{2V}\Big/\delta \end{array}\right| = \left|\begin{array}{c} \left|C_m^{*}\right| \\ \hline F \end{array}\right| \tag{28}$$

where the submatrices are given by

$$\left[A_{ml}^*\right] = \left[\left(G_L\right)_{mj}\right]\left[\ S\ \right]\left[\left(\beta c_{l_\theta}\right)_{jk}\right]\left[\ S\ \right]\left[\ D\ \right]\left[T_{kl}\right] +$$

$$c\left[\left(G_M\right)_{mj}\right]\left[\ S\ \right]\left[\left(\beta c_{m_\theta}\right)_{jk}\right]\left[\ S\ \right]\left[\ D\ \right]\left[T_{kl}\right]$$

$$\left|B_m^*\right| = -\left[\left(G_L\right)_{mj}\right]\left[\ S\ \right]\left|\left(\beta c_{l_p}\right)_j\right| - c\left[\left(G_M\right)_{mj}\right]\left[\ S\ \right]\left|\left(\beta c_{m_p}\right)_j\right|$$

$$\left|C_m^*\right| = \left[\left(G_L\right)_{mj}\right]\left[\ S\ \right]\left|\left(\beta c_{l_\delta}\right)_j\right| + c\left[\left(G_M\right)_{mj}\right]\left[\ S\ \right]\left|\left(\beta c_{m_\delta}\right)_j\right|$$

$$\left[D_l^*\right] = -\left[al + y_j\right]\left[\ S\ \right]\left[\left(\beta c_{l_\theta}\right)_{jk}\right]\left[\ S\ \right]\left[\ D\ \right]\left[T_{kl}\right]$$

$$E = -\left[al + y_j\right]\left[\ S\ \right]\left|\left(\beta c_{l_p}\right)_j\right|$$

$$F = \left[al + y_j\right]\left[\ S\ \right]\left|\left(\beta c_{l_\delta}\right)_j\right|$$

Note that the subscripts j and k assume all values, both even and odd, and the subscripts m and l assume only the even values.

The analogous partitioned matrix equation to be used when the rate-of-twist influence functions are known is

$$\left[\begin{array}{c|c} \frac{1}{\frac{qc}{\beta}}\left[\ I\ \right] - \left[\overline{A_{ml}^{*}}\right] & \left|B_m^{*}\right| \\ \hline \left\lfloor\ \overline{D_l^{*}}\ \right\rfloor & E \end{array}\right] \left|\begin{array}{c} \left|\frac{\left(\frac{d\theta}{dy}\right)_l}{\delta}\right| \\ \hline \frac{pb}{2V}\Big/\delta \end{array}\right| = \left|\begin{array}{c} \left|\overline{C_m^{*}}\right| \\ \hline F \end{array}\right| \tag{29}$$

where the submatrices are given by

$$\left[\overline{A_{ml}^{*}}\right] = \left[\left(\frac{\partial G_L}{\partial y}\right)_{mj}\right]\left[\ S\ \right]\left[\left(\beta c_{l_\theta}\right)_{jk}\right]\left[\ S\ \right]\left[T_{kl}\right] + c\left[\left(\frac{\partial G_M}{\partial y}\right)_{mj}\right]\left[\ S\ \right]\left[\left(\beta c_{m_\theta}\right)_{jk}\right]\left[\ S\ \right]\left[T_{kl}\right]$$

$$\left|\overline{B_m^{*}}\right| = -\left[\left(\frac{\partial G_L}{\partial y}\right)_{mj}\right]\left[\ S\ \right]\left|\left(\beta c_{l_p}\right)_j\right| - c\left[\left(\frac{\partial G_M}{\partial y}\right)_{mj}\right]\left[\ S\ \right]\left|\left(\beta c_{m_p}\right)_j\right|$$

$$\left|\overline{C_m^{*}}\right| = \left[\left(\frac{\partial G_L}{\partial y}\right)_{mj}\right]\left[\ S\ \right]\left|\left(\beta c_{l_\delta}\right)_j\right| + c\left[\left(\frac{\partial G_M}{\partial y}\right)_{mj}\right]\left[\ S\ \right]\left|\left(\beta c_{m_\delta}\right)_j\right|$$

$$\left\lfloor\ \overline{D_l^{*}}\ \right\rfloor = -\left\lfloor a_l + y_j\right\rfloor\left[\ S\ \right]\left[\left(\beta c_{l_\theta}\right)_{jk}\right]\left[\ S\ \right]\left[T_{kl}\right]$$

The scalars E and F are given after equation (28). Here again the subscripts j and k take on all values, whereas m and l assume only even values.

The aileron-reversal equations may also be expressed in this reduced-order form. Thus, equation (14), in matrix form, is

$$\left|\theta_k\right| = \frac{q_{rev}c}{\beta}\left[\left[A_{ml}^*\right] + \frac{1}{F}\left|C_m^*\right|\left\lfloor D_l^*\right\rfloor\right]\left|\theta_l\right| \tag{30}$$

The submatrices are defined after equation (28). Similarly, equation (15) becomes

$$\left|\left(\frac{d\theta}{dy}\right)_m\right| = \frac{q_{rev}c}{\beta}\left[\left[\overline{A_{ml}^*}\right] + \frac{1}{F}\left|\overline{C_m^*}\right|\left\lfloor \overline{D_l^*}\right\rfloor\right]\left|\left(\frac{d\theta}{dy}\right)_l\right| \tag{31}$$

The submatrices in this case are given immediately after equation (29). Again, standard matrix iteration procedure may be used to solve equation (30) or (31), the amount of work being approximately one-fourth as much as is involved in the iteration of equation (25) or (26).

Simplifications for Wings With an Elastic Axis

Two operations are required to modify the aeroelastic matrix equations when an elastic axis exists. First, all terms involving the matrices $\left[G_L\right]$ or $\left[\frac{\partial G_L}{\partial y}\right]$ are deleted. Second, the section-moment-coefficient matrices $\left[\beta c_{m_\theta}\right]$, $\left|\beta c_{m_p}\right|$, and $\left|\beta c_{m_\delta}\right|$ are replaced by $\left[\beta c_{q_\theta}\right]$, $\left|\beta c_{q_p}\right|$, and $\left|\beta c_{q_\delta}\right|$ in accordance with equation (17).

Computational Procedure

As has been previously mentioned, the task of calculating the rolling effectiveness for the given configuration flying at a given altitude and speed is straightforward; only the solution of a set of simultaneous equations is necessary. If a complete knowledge of the aeroelastic behavior over large ranges of speed and altitude is desired, however, the manner in which the various parameters are involved should be taken into account in determining the sequence of calculations. It should be noted that the Mach number enters the problem in a complicated manner, whereas the dependence on altitude is rather simple; that is, the Mach number affects the aerodynamic matrices and the altitude affects only the dynamic pressure q. It is therefore obvious that the most economical way to perform the computations is to calculate the variation of rolling effectiveness with dynamic pressure for several constant values of Mach number. In addition, since the rolling effectiveness is of little interest when the controls are reversed, the range of dynamic pressures should be restricted to values less than q_{rev}. The dynamic pressure at reversal should, therefore, be determined for each value of Mach number before proceeding with the calculation of rolling effectiveness.

An outline of the steps required in the determination of the aeroelastic effect on roll for a range of altitude and Mach number is included herein. For simplicity, only one of the several numerical approaches derived in this section - that is, the one wherein the twist influence functions G_L and G_M and the interpolation procedure are utilized - is illustrated; the others follow the same outline, differing only in detail.

(1) Evaluate, either analytically or experimentally, the twist influence functions $G_L(y,\eta)$ and $G_M(y,\eta)$ at stations $y/l = 0, 0.2, 0.4, \ldots 1.0$ due to loads and torques applied at stations $\eta/l = 0, 0.1, 0.2, \ldots 1.0$. From these values, form the 11-by-6 matrices $\left[(G_L)_{mj}\right]$ and $\left[(G_M)_{mj}\right]$.

(2) For a given Mach number (one should be chosen which results in a value of $\beta l/c$ which appears in the tables) determine the indicial section lift and moment coefficients βc_{l_θ} and βc_{m_θ}. These coefficients, which are found by applying equation (7) to the values of $\beta c_{l_\theta}'$ and $\beta c_{m_\theta}'$ in table I, can then be used to form the square matrices $\left[(\beta c_{l_\theta})_{jk}\right]$ and $\left[(\beta c_{m_\theta})_{jk}\right]$.

(3) In a similar manner, form the column matrices $\left|\left(\beta c_{l_p}\right)_j\right|$ and $\left|\left(\beta c_{m_p}\right)_j\right|$, making use of equation (9) in conjunction with the values of $\beta c_{l_{p_o}}$ and βc_{l_α} in table II.

(4) Determine the section loading coefficients due to a unit aileron deflection. Use these coefficients to construct the column matrices $\left|\left(\beta c_{l_\delta}\right)_j\right|$ and $\left|\left(\beta c_{m_\delta}\right)_j\right|$. (These coefficients are listed for one aileron configuration in table III. Equations for the coefficients for a rather general aileron configuration are included in appendix B.)

(5) Compute the matrices $\left[A_{ml}^*\right]$, $\left|B_m^*\right|$, $\left|C_m^*\right|$, and $\left[D_l^*\right]$ and the scalars E and F defined immediately after equation (28). The integrating and differentiating matrices $\left[S\right]$ and $\left[D\right]$ in these definitions are given by equations (18) and (19); the interpolating matrix $\left[T_{kl}\right]$ is given by equation (27); the row matrix $\left|al + y_j\right|$ is made up of the moment arms about the rolling axis.

(6) Form the matrix $\left[A_{ml}^*\right] + \frac{1}{F}\left|C_m^*\right|\left[D_l^*\right]$.

(7) Obtain q_{rev} by iterating this matrix (see eq. (30)).

(8) For each of several values of q between zero and q_{rev}, form the matrix equation (28). Solution of this equation yields $\left(\frac{pb}{2V}\middle/\delta\right)_F$ for each value of q. Obtain the rolling effectiveness ϕ by dividing $\left(\frac{pb}{2V}\middle/\delta\right)_F$ by $\left(\frac{pb}{2V}\middle/\delta\right)_R$ $\left(\left(\frac{pb}{2V}\middle/\delta\right)_R = \frac{F}{E}\right)$.

(9) Repeat steps (2) to (8) for several other values of Mach number.

SAMPLE APPLICATION

In this section, aileron effectiveness and reversal speed are found for a specific aircraft by the approach set forth in this paper, which is termed "lifting surface theory," and by two simplified methods. Each half

of the exposed wing consists of a uniformly thick aluminum plate with an aspect ratio l/c of 3/2 and a thickness ratio t/c of 0.02. The full-span aileron is formed by bending the plate along the 0.8-chord line; therefore $b_a/l = 1.0$ and $c_a/c = 0.2$. The wings are mounted rigidly on the body, which has a radius of one-fifth the exposed wing semispan; therefore $a = 0.2$. These ratios are sufficient to define completely the configuration, since, as is seen later, the results are independent of absolute dimensions.

Although the plate is considered to be bent in order to form the aileron, the plate is assumed to behave structurally as if no bend had been made. On the basis of this assumption the necessary structural influence coefficients are determined in appendix A by means of a simplified flat-plate theory. In this case, as could be expected, not only does an elastic axis exist but also this elastic axis coincides with the midchord.

Calculation by Lifting-Surface Theory

Since the influence functions are obtained analytically, the rate-of-twist influence function rather than the twist influence function has been determined in order that no numerical differentiation be necessary. In addition, the wing structure being free of discontinuities, the interpolation procedure developed in the preceding section may be successfully employed. Equations (29) and (31), modified as outlined in the preceding section, are therefore used to compute $\frac{pb}{2V}\Big/\delta$ and q_{rev}, respectively.

Before proceeding with the solution of equations (29) and (31), the dimensional character of the structural, aerodynamic, integrating, and interpolating matrices involved in these equations should be considered. The aerodynamic and interpolating matrices are clearly dimensionless. The integrating matrix $\left[S\right]$ and the rolling-moment-arm matrix $\left[al + y_j\right]$ are proportional to the exposed semispan l. The influence-function matrix for the example configuration, which is presented in table IV, is written as the product of the quantity $l\Big/\frac{Gt^3c}{3}$ and a nondimensional matrix.

The aforementioned independence of absolute dimensions can now be demonstrated. Equations (29) and (31) can be written in the form

$$\left[\begin{array}{c|c} \dfrac{Gt^3/3l^2}{qc/\beta}\left[\ I\ \right] - \dfrac{Gt^3}{3l^2}\left[\overline{A_{ml}^*}\right] & \dfrac{Gt^3}{l}\left|\overline{B_m^*}\right| \\ \hline \dfrac{1}{l^3}\left|\overline{D_l^*}\right| & \dfrac{E}{l^2} \end{array}\right] \left|\begin{array}{c} \left|\dfrac{d\theta_l}{d\frac{y}{l}}\Big/\delta\right| \\ \hline -\dfrac{pb}{2V}\Big/\delta \end{array}\right| = \left|\begin{array}{c} \dfrac{Gt^3}{3l}\left|\overline{C_m^*}\right| \\ \hline \dfrac{F}{l^2} \end{array}\right| \tag{32}$$

and

$$\left|\frac{d\theta_m}{d\frac{y}{l}}\right| = \frac{q_{rev}cl^2}{\beta\frac{Gt^3}{3}}\left[\frac{Gt^3}{3l^2}\left[\overline{A_{ml}^*}\right] + \frac{Gt^3}{3l}\left|\overline{C_m^*}\right|\frac{1}{Fl}\left|\overline{D_l^*}\right|\right]\left|\frac{d\theta_l}{d\frac{y}{l}}\right| \tag{33}$$

where the multiplication of the various submatrices by the indicated quantities yields nondimensional results. Inspection of equations (32) and (33) shows that only ratios of the dimensions are involved, and that the quantity

$$\frac{qcl^2}{\beta\frac{Gt^3}{3}}$$

is an important nondimensional parameter for this particular configuration.

The step-by-step procedure previously outlined has been followed for the example configuration and the results are included in figure 3. Since the dynamic pressure in this case is essentially an altitude parameter, the results in figure 3 are shown plotted against the pressure ratio P_h/P_0, where P_0 is the standard pressure at sea level, as obtained from reference 5, and P_h is the free-stream static pressure at altitude and is related to q by the equation

$$P_h = \frac{2q}{\gamma M^2}$$

in which γ is the ratio of specific heats of air.

Simplified Methods

Two simplified methods of analysis have also been used to solve for q_{rev} and ϕ for the example. They differ from the method previously described only in that the airloads are determined by simplified means. In the first method, lifting-surface theory is modified in a manner similar to that used in reference 6, wherein it is assumed that the chordwise center of pressure due to structural deformation and roll coincides with the elastic axis of the wing. Thus, the total twisting moment about the elastic axis is equal to the twisting moment due to only the aileron, and equation (15) becomes

$$\frac{d\theta}{dy} = \frac{qc^2}{\beta}\delta\int_0^l \frac{\partial c_M(y,\eta)}{\partial y}\beta c_{m_\delta}(\eta)\,d\eta \qquad (34)$$

The rolling-moment equation, equation (12), is unchanged. A solution to the problem has been obtained by using matrices in a manner similar to that employed previously. In this case, however, $d\theta/dy$ is given explicitly by equation (34) and, therefore, $\frac{pb}{2V}\Big/\delta$ can be calculated directly, the solution of a set of simultaneous equations being unnecessary.

In the second method of analysis, the aerodynamic terms are derived on the basis of two-dimensional (strip) theory. For the case wherein the elastic axis lies on the midchord, the center of pressure due to structural deformation and roll coincides with the elastic axis of the wing and the only twisting moment about the elastic axis is that produced by the aileron. Therefore, equation (34) expresses $d\theta/dy$ exactly, and the rolling rate obtained by solving equations (12) and (34) is exact. Because of the simplicity of the strip theory, these calculations can be performed analytically.

The results obtained by using these methods, termed, respectively, "modified lifting-surface theory" and "strip theory," are also shown in figure 3 for comparison with the results obtained by using lifting-surface theory.

RESULTS AND DISCUSSION

The results shown in figure 3 indicate that the variation of rolling effectiveness ϕ with the pressure ratio P_h/P_0 is, for practical purposes, linear. This linearity suggests the possibility that, for configurations of the type considered, only the computation of pressure ratio at

reversal $(P_h/P_0)_{rev}$ would be required; the rolling effectiveness for smaller values of P_h/P_0 could then be obtained by linear interpolation. In this way the computation time could be greatly reduced, the calculation of $(P_h/P_0)_{rev}$ being a relatively simple process. Some care should be taken, however, in making use of this linearity, since it appears to depend on the proximity of the elastic axis to the chordwise center of pressure due to angle of attack. For wings wherein the elastic axis is distant from this center of pressure, considerable curvature of the rolling-effectiveness curves could result. At the other extreme, the results in figure 3 obtained by using the two simplified methods are exactly linear, since, in both cases, the elastic axis and the center of pressure are coincident.

An additional consequence of this linearity is that the accuracy with which a particular method predicts $(P_h/P_0)_{rev}$ is a direct measure of its ability to predict rolling effectiveness. A comparison of the values of $(P_h/P_0)_{rev}$ obtained by the two simplified methods with those obtained by the method presented in this paper is therefore shown in figure 4, wherein $(P_h/P_0)_{rev}$ is plotted against Mach number. Although the results show very little difference in the values of $(P_h/P_0)_{rev}$ as obtained by the three methods at high values of M, considerable difference exists at low values of M. The results obtained by the use of the modified lifting-surface theory are consistently unconservative; the results obtained by the use of strip theory are consistently conservative. Modified lifting-surface theory neglects the twisting moments arising from the twist of the wing; only the torques caused by aileron deflection are considered. Neglect of the twisting moments due to angle-of-attack changes evidently reduces the resultant angle of twist and therefore reduces the adverse rolling moments caused by the deformation. When strip theory is used, the elastic twist is again lower than that obtained by lifting-surface theory because, again, only the twisting moments caused by the aileron deflection are present. Here, however, the absence of the finite-span effects actually results in a greater adverse rolling moment, even though the twist causing the adverse rolling moment is in itself smaller.

Further mention should be made of the behavior at large Mach numbers. Actually all three methods should yield the same results as M approaches infinity because, as M increases indefinitely, lifting-surface theory approaches strip theory. As an illustration of this fact, the rate of roll for a rigid wing $\left(\frac{pb}{2V}\Big/\delta\right)_R$ is shown as a function of M in figure 5. The values of $\left(\frac{pb}{2V}\Big/\delta\right)_R$ obtained by using lifting-surface theory rapidly

approach the values obtained by using strip theory as the Mach number increases. Thus, at high values of M the use of strip theory should yield aeroelastic solutions of an accuracy comparable to that obtained by using lifting-surface theory.

In actual application it may be convenient to have rolling effectiveness given as a plot of pressure ratio against Mach number for constant values of rolling effectiveness. A graph of this type may be made by cross-plotting the information contained in figure 3 and is included in figure 6. Also included in figure 6 is an additional ordinate that gives the altitude as obtained from the standard-atmosphere table in reference 5.

The rolling effectiveness ϕ at any time during a particular flight may be determined as a function of Mach number if a history of the flight is known in the form of a plot of standard altitude against Mach number. For example, consider two constant-altitude flights, one at 30,000 feet and the other at 20,000 feet. The resulting variation of the rolling effectiveness of the example configuration with Mach number is shown in figure 7.

The indicial-solution (aerodynamic-influence-function) approach used herein in the calculation of the aerodynamic loads exhibits considerable promise of being applicable to plan forms other than rectangular. The delta wing and the low-aspect-ratio swept wing at supersonic speeds can be handled in the same way as the rectangular wing; care should be taken in these cases, however, to account for chordwise bending where necessary. Other static aeroelastic problems such as center-of-pressure shift (which has been considered by Frick and Chubb in ref. 1 for high-aspect-ratio swept wings) and load distribution seem to be amenable to analysis by the methods contained herein. It might even be possible to extend the approach to take into account unsteady aerodynamic effects and thereby to obtain accurate solutions to flutter problems. The calculations in the last case would undoubtedly be arduous and the main usefulness of the approach would be to establish a basis for the evaluation of more practical but necessarily less accurate solutions of the flutter problem.

Problems involving configurations about which the flow is not substantially potential are generally not amenable to this type of approach. More specifically, the success of the approach depends on the applicability of linearization to the aerodynamics and on the ability to calculate the necessary indicial load distributions.

CONCLUDING REMARKS

A method has been developed for the prediction of the aeroelastic effects on the roll of rectangular wings in supersonic flow. The method

is based on the use of influence functions, either analytically or experimentally obtained, to calculate the structural distortion due to airloads. The airloads, themselves, are calculated on the basis of linearized lifting-surface theory by superposing basic airloads resulting from elementary angle-of-attack distributions. The solution of the aeroelastic equations has been obtained by means of a numerical procedure suitable for use with desk-type calculators.

Results for an example configuration indicate that the variation of rolling effectiveness with the free-stream static pressure at a constant Mach number is almost linear; a good approximation may be made by assuming a linear variation. Thus, in any other cases wherein this linearity can be expected - that is, when the elastic axis is near the center of pressure due to angle of attack - the calculations may be greatly simplified in that it is necessary to compute only the free-stream static pressure at aileron reversal.

The results obtained by using the method of analysis presented in this paper are compared with the results obtained by using simplified methods of analysis. Although aerodynamic strip theory is valid at high Mach numbers, too conservative results are obtained at low supersonic Mach numbers because of neglect of finite-span effects. A modified lifting-surface theory, in which twisting moments due to structural deformation and roll have been neglected, yields results which are unconservative at low supersonic Mach numbers.

Langley Aeronautical Laboratory,
National Advisory Committee for Aeronautics,
Langley Field, Va., December 2, 1953.

APPENDIX A

STRUCTURAL ANALYSIS OF THE EXAMPLE CONFIGURATION

The deformations of the wing of the example configuration are analyzed herein by using the approximate plate theory presented in references 4 and 7. This method expresses the deflection w of a plate at any point (x,y) in the form $w(x,y) = W(y) - x\,\theta(y)$ where $W(y)$ is the deflection of the wing at the midchord and $\theta(y)$ is the twist of the wing. (See fig. 1.) An energy solution of the problem is used wherein the expression for the potential energy of the plate is written in terms of the approximate deflection function. Minimization of this potential-energy expression yields two ordinary differential equations in $W(y)$ and $\theta(y)$. Since the deflection $W(y)$ has no effect on the airload, it is eliminated from the two equations; the process yields a single equation in $\theta(y)$. This equation has been derived in reference 7 (eq. (A22) of that paper) and for a rectangular cantilever plate of constant thickness t becomes, in the notation of the present paper,

$$\frac{Dc^3}{12}\frac{d^3\theta}{dy^3} - 2(1 - \mu)Dc\frac{d\theta}{dy} = -\int_y^l M(\zeta)\,d\zeta \tag{A1}$$

with the boundary conditions

$$\theta(0) = \frac{d\theta(0)}{dy} = \frac{d^2\theta(l)}{dy^2} = 0$$

In equation (A1), D is the plate stiffness:

$$D = \frac{Et^3}{12(1 - \mu^2)}$$

where E is Young's modulus and μ is Poisson's ratio. As could be expected for this structure, the twists are seen to be dependent solely on the twisting moment about the midchord $M(y)$.

The solution to equation (A1) for a general $M(y)$ can be obtained by superposing indicial solutions found by considering the moment to be

concentrated at any spanwise station η. Thus, let

$$M(y) = \delta(y - \eta)$$

where $\delta(y - \eta)$ is the Dirac delta function.

Equation (A1) now becomes

$$\frac{Dc^3}{12}\frac{\partial^3 G_M(y,\eta)}{\partial y^3} - 2(1 - \mu)Dc\frac{\partial G_M(y,\eta)}{\partial y} = -1(\eta - y) \qquad (A2)$$

where $1(\eta - y)$ is the unit step function:

$$1(\eta - y) = 1 \qquad (y \leq \eta)$$

$$1(\eta - y) = 0 \qquad (y > \eta)$$

The rate-of-twist influence function $\frac{\partial G_M(y,\eta)}{\partial y}$ is the quantity required in order to obtain the rate of twist by superposition. This quantity is

$$\left.\begin{aligned} \frac{\partial G_M(y,\eta)}{\partial y} &= \frac{12l^2}{Dc^3\lambda^2}\frac{1}{\cosh\lambda}\left[\cosh\lambda - \cosh\lambda\left(1 - \frac{y}{l}\right) - \right. \\ &\qquad \left. \sinh\lambda\left(1 - \frac{\eta}{l}\right)\sinh\lambda\frac{y}{l}\right] \qquad (y \leq \eta) \\ \frac{\partial G_M(y,\eta)}{\partial y} &= \frac{12l^2}{Dc^3\lambda^2}\frac{\cosh\lambda\left(1 - \frac{y}{l}\right)}{\cosh\lambda}\left(-1 + \cosh\lambda\frac{\eta}{l}\right) \qquad (y > \eta) \end{aligned}\right\} \qquad (A3)$$

where

$$\lambda = \frac{l}{c}\sqrt{24(1 - \mu)}$$

With regard to this solution, it should be noted that the quantity $12l^2/Dc^3\lambda^2$ can be written in the form $1\Big/\frac{Gt^3c}{3}$, where G is the shear modulus of elasticity of the material.

Superposition of the rate-of-twist influence function yields

$$\frac{d\theta(y)}{dy} = \int_0^l \frac{\partial G_M(y,\eta)}{\partial y} M(\eta)\, d\eta \tag{A4}$$

Values of $\partial G_M/\partial y$ for $l/c = 3/2$ and $\mu = 1/3$ (which yields $\lambda = 6$) have been computed for $0 \leqq \frac{y}{l} \leqq 1$ in intervals of 0.2 and $0 \leqq \frac{\eta}{l} \leqq 1$ in intervals of 0.1; the results are included in matrix form in table IV.

APPENDIX B

DERIVATION OF AERODYNAMIC COEFFICIENTS

In this appendix the aerodynamic loads necessary for computing rolling effectiveness are derived. The loads are found in the form of section lift and moment coefficients by applying linearized supersonic lifting-surface theory to the rectangular wing with three different angle-of-attack distributions: the unit-step angle-of-attack distribution shown in figure 2(c), the angle-of-attack distribution caused by rolling, and the angle-of-attack distribution resulting from aileron deflection.

Analyses of each of these problems are contained in the literature. The unit-step problem is essentially the same as the problem of finding the loads due to deflection of an outboard aileron, which has already been solved (see, for example, ref. 8); the rolling problem has been treated by many investigators (see, for example, ref. 9). There does not seem to be any report, however, that gives the desired coefficients in a form sufficiently complete for the purposes of this paper. For this reason and also for convenience, the necessary aerodynamic quantities are derived completely herein.

When linearized lifting-surface theory is used, the lift per unit area of a thin wing is given by

$$p(x,y) = \frac{4q}{V} \frac{\partial \varphi(x,y)}{\partial x} \tag{B1}$$

where x is positive in the direction of the airstream. The potential φ, evaluated at the surface of the wing, is

$$\varphi(x,y) = \frac{V}{\pi} \iint_S \frac{\sigma(\xi,\zeta)\, d\xi\, d\zeta}{\sqrt{(\xi - x)^2 - \beta^2(\zeta - y)^2}} \tag{B2}$$

where $\sigma(\xi,\zeta)$ is the local angle of attack of the wing. In general, for a rectangular wing, the region of integration S includes the entire area on the wing within the forward Mach cone from the point (x,y). However, in order to obtain the potential at a point near a wing tip, the proper region of integration S is determined by using Evvard's method (ref.10).

The spanwise loading and twisting moment about the midchord are given by

$$\left.\begin{aligned} L(y) &= \int_{-c/2}^{c/2} p(x,y)\ dx \\ M(y) &= -\int_{-c/2}^{c/2} x\ p(x,y)\ dx \end{aligned}\right\} \tag{B3}$$

If the expression for $p(x,y)$ is substituted into equations (B3), and the results are integrated, the lift and moment become:

$$\left.\begin{aligned} L(y) &= \frac{4q}{V}\,\varphi\left(\frac{c}{2},y\right) \\ M(y) &= -\frac{4q}{V}\left[\frac{c}{2}\,\varphi\left(\frac{c}{2},y\right) - \int_{-c/2}^{c/2} \varphi(x,y)\ dx\right] \end{aligned}\right\} \tag{B4}$$

where the fact that the potential is zero at the leading edge has been taken into account.

The foregoing equations can be nondimensionalized by letting

$$\beta c_l = \frac{L\beta}{qc}$$

$$\beta c_m = \frac{M\beta}{qc^2}$$

$$x_1 = \frac{1}{2} + \frac{x}{c}$$

$$y_1 = 1 - \frac{y}{l}$$

$$\Phi = \frac{\pi}{Vl}\,\varphi$$

The resulting equations are

$$\left.\begin{aligned} \beta c_{l}(y_1) &= \frac{4m}{\pi}\,\Phi(1,y_1) \\ \beta c_{m}(y_1) &= -\frac{4m}{\pi}\left[\frac{1}{2}\,\Phi(1,y_1) - \int_0^1 \Phi(x_1,y_1)\,dx_1\right] \end{aligned}\right\} \tag{B5}$$

where

$$\Phi(x_1,y_1) = \iint_S \frac{\sigma(\xi_1,\zeta_1)\,d\zeta_1\,d\xi_1}{\sqrt{(x_1-\xi_1)^2 - m^2(y_1-\zeta)^2}} \tag{B6}$$

and m is the modified aspect-ratio parameter $\beta l/c$.

Derivation of $\beta c_{l_\theta}'$ and $\beta c_{m_\theta}'$

The equations for the spanwise loading $\beta c_{l_\theta}'$ and the twisting moment about the midchord $\beta c_{m_\theta}'$ due to the unit-step angle-of-attack distribution shown in figure 2(c) become, from equations (B5),

$$\left.\begin{aligned} \beta c_{l_\theta}'(y_1,\eta_1) &= \frac{4m}{\pi}\,\Phi(1,y_1,\eta_1) \\ \beta c_{m_\theta}'(y_1,\eta_1) &= -\frac{4m}{\pi}\left[\frac{1}{2}\,\Phi(1,y_1,\eta_1) - \int_0^1 \Phi(x_1,y_1,\eta_1)\,dx_1\right] \end{aligned}\right\} \tag{B7}$$

where the potential Φ is found for an angle-of-attack distribution defined by the unit step function:

$$\sigma(y_1,\eta_1) = 1(\eta_1 - y_1)$$

or

$$\sigma(y_1,\eta_1) = 1 \qquad (\eta_1 \geqq y_1)$$

$$\sigma(y_1,\eta_1) = 0 \qquad (\eta_1 < y_1)$$

Equation (B6) becomes

$$\Phi(x_1,y_1,\eta_1) = \iint_{\Sigma} \frac{d\zeta_1\, d\xi_1}{\sqrt{(x_1 - \xi_1)^2 - m^2(y_1 - \zeta_1)^2}} \tag{B8}$$

The region of integration Σ includes only that portion of S which lies within the region of the wing between the wing tip and the position of the unit step in angle of attack at η_1.

The plan form and angle-of-attack distribution considered are those shown in figure 2(c). From this figure it can be seen that the position of the unit step is restricted to the range $0 \leqq \eta_1 \leqq 1$. If, in addition, the modified aspect-ratio parameter m is restricted to values greater than $\frac{1}{1 + 2a}$, the potentials Φ for the finite wing in figure 2(c) are exactly the same as the potentials on the finite wing portion of the following semi-infinite plan form which has been obtained by allowing the left tip and the trailing edge of the finite wing to approach infinity:

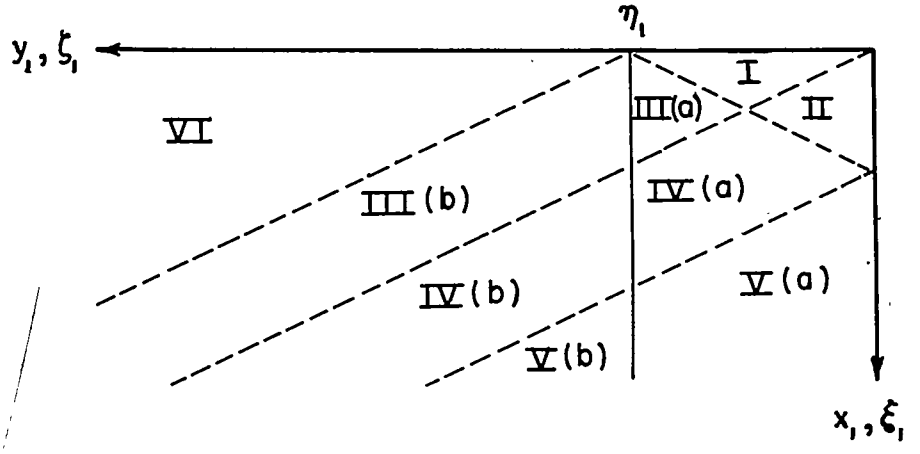

Thus, attention is confined to the derivation of the potentials on this semi-infinite plan form. With the potentials known, the loading coefficients on the finite wing are given by equations (B7).

The Mach lines shown in the above sketch bound a number of distinct regions. These regions are significant because the area of integration in equation (B8) takes a different geometric form in each; it is to be expected, therefore, that the potential Φ is given by a different equation in each region. The proper area of integration Σ (shown

shaded) and the potential Φ for the various regions, as found from equation (B8), are:

In region I:

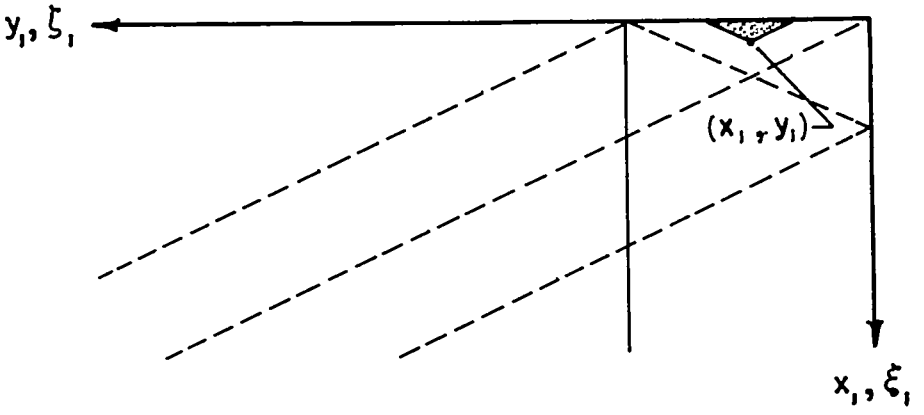

$$\Phi_I = \frac{\pi}{m} x_1$$

In region II:

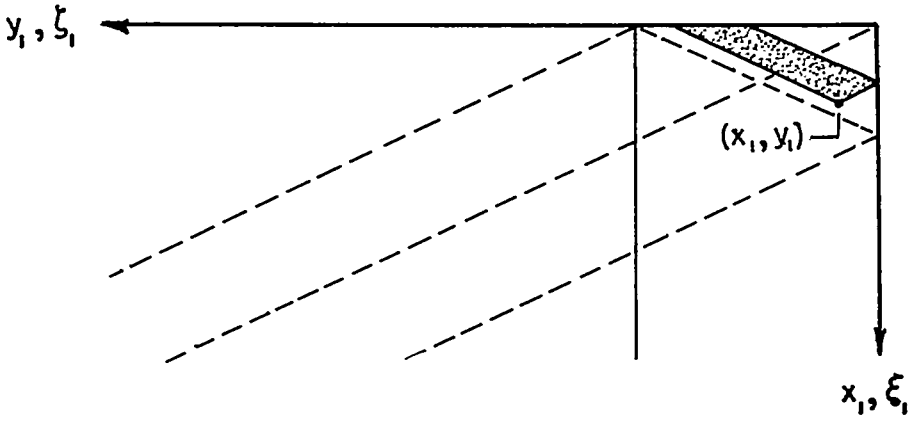

$$\Phi_{II} = \frac{2}{m}\left(\sqrt{my_1}\sqrt{x_1 - my_1} + x_1 \tan^{-1}\sqrt{\frac{my_1}{x_1 - my_1}}\right)$$

In region III(A):

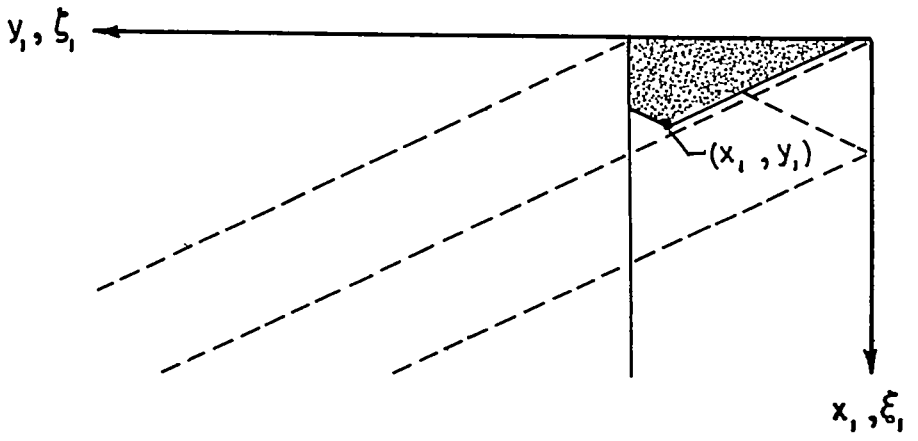

$$\Phi_{III(A)} = \frac{2}{m}\left[x_1 \tan^{-1}\sqrt{\frac{x_1 + m(\eta_1 - y_1)}{x_1 - m(\eta_1 - y_1)}} + m(\eta_1 - y_1)\tanh^{-1}\sqrt{\frac{x_1 - m(\eta_1 - y_1)}{x_1 + m(\eta_1 - y_1)}}\right]$$

In region III(B):

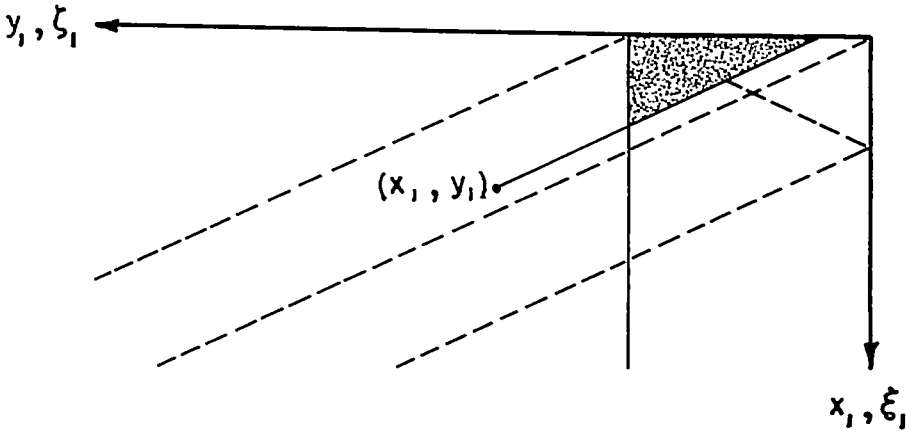

$$\Phi_{III(B)} = \frac{2}{m}\left[x_1 \tan^{-1}\sqrt{\frac{x_1 + m(\eta_1 - y_1)}{x_1 - m(\eta_1 - y_1)}} + m(\eta_1 - y_1)\tanh^{-1}\sqrt{\frac{x_1 + m(\eta_1 - y_1)}{x_1 - m(\eta_1 - y_1)}}\right]$$

Notice that the only difference in the equations for $\Phi_{III(A)}$ and $\Phi_{III(B)}$ is that the radical in the inverse-hyperbolic-tangent term in the equation for $\Phi_{III(A)}$ is the reciprocal of the radical in the corresponding term in the equation for $\Phi_{III(B)}$. Thus, the following form holds for both regions:

$$\Phi_{III} = \frac{2}{m}\left[x_1 \tan^{-1}\sqrt{\frac{x_1 + m(\eta_1 - y_1)}{x_1 - m(\eta_1 - y_1)}} + m(\eta_1 - y_1)\tanh^{-1}k_1\right]$$

where

$$k_1 = \sqrt{\frac{x_1 - m(\eta_1 - y_1)}{x_1 + m(\eta_1 - y_1)}} \qquad \left(y_1 \leqq \eta_1\right)$$

$$k_1 = \sqrt{\frac{x_1 + m(\eta_1 - y_1)}{x_1 - m(\eta_1 - y_1)}} \qquad \left(y_1 \geqq \eta_1\right)$$

A similar situation occurs in the derivation of $\Phi_{IV(A)}$ and $\Phi_{IV(B)}$ and of $\Phi_{V(A)}$ and $\Phi_{V(B)}$. Therefore, the equations for Φ_{IV} and Φ_{V} may be derived for either the subregion (A) or (B) and applied throughout the entire region.

In region IV:

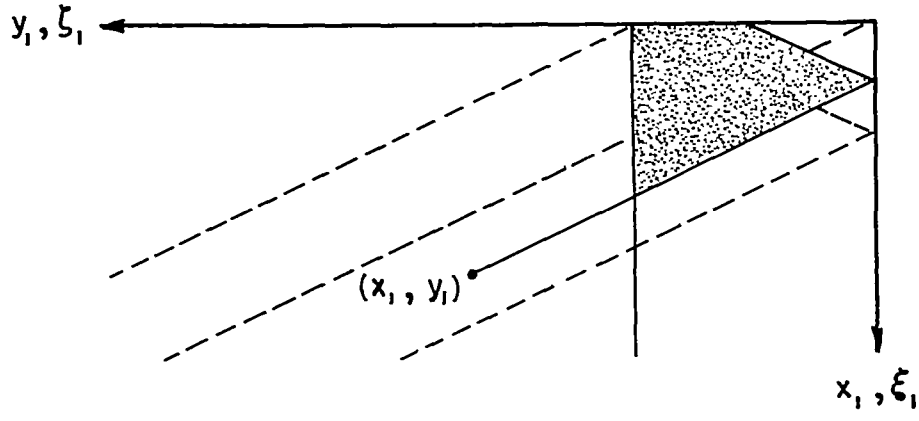

$$\Phi_{IV} = \frac{2}{m}\left\{\sqrt{my_1}\sqrt{x_1 - my_1} + x_1\left[\tan^{-1}\sqrt{\frac{x_1 + m(\eta_1 - y_1)}{x_1 - m(\eta_1 - y_1)}} - \tan^{-1}\sqrt{\frac{x_1 - my_1}{my_1}}\right] + m(\eta_1 - y_1)\tanh^{-1}k_1\right\}$$

In region V:

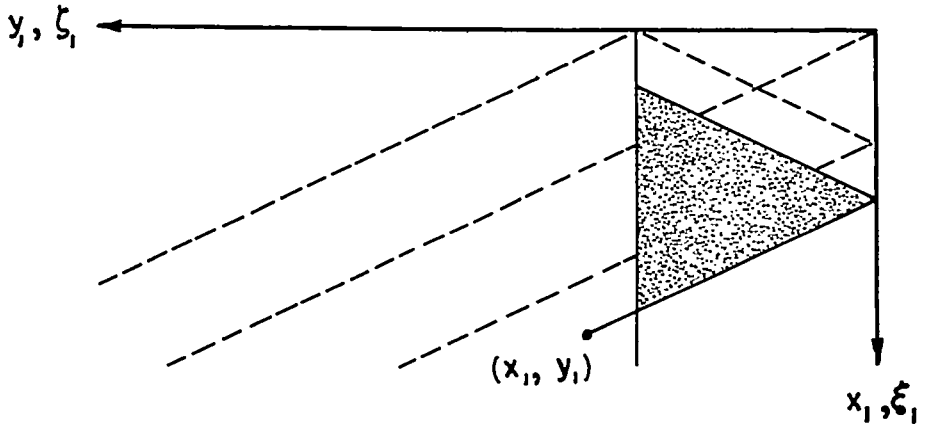

$$\Phi_V = \frac{2}{m}\left[\sqrt{m\eta_1}\sqrt{my_1} + m(\eta_1 - y_1)\tanh^{-1}k_2\right]$$

where

$$k_2 = \sqrt{y_1/\eta_1} \qquad \left(y_1 \leqq \eta_1\right)$$

$$k_2 = \sqrt{\eta_1/y_1} \qquad \left(y_1 \geqq \eta_1\right)$$

In region VI:

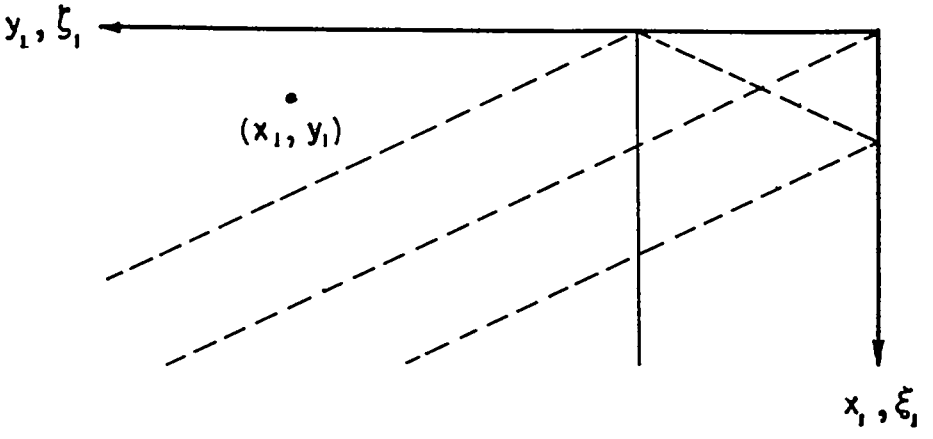

$$\Phi_{VI} = 0$$

Since the spanwise loading $\beta c_{l_\theta}'$ is determined by the value of Φ at the trailing edge (see eq. (B7)), the equation for $\beta c_{l_\theta}'$ is dependent only on the region that the trailing edge is in. For example, if for a given value of y_1 the trailing edge is in region III, the value of $\beta c_{l_\theta}'$ is

$$\left[\beta c_{l_\theta}'(y_1,\eta_1)\right]_{III} = \frac{4m}{\pi}\Phi_{III}(y_1,1,\eta_1)$$

Thus, the equations for $\beta c_{l_\theta}'$ are:

$$\left.\begin{aligned}
\left(\beta c_{l_\theta}'\right)_I &= 4 \\
\left(\beta c_{l_\theta}'\right)_{II} &= \frac{8}{\pi}\left(\sqrt{my_1}\sqrt{1 - my_1} + \tan^{-1}\sqrt{\frac{my_1}{1 - my_1}}\right) \\
\left(\beta c_{l_\theta}'\right)_{III} &= \frac{8}{\pi}\left[\tan^{-1}\sqrt{\frac{1 + m(\eta_1 - y_1)}{1 - m(\eta_1 - y_1)}} + m(\eta_1 - y_1)\tanh^{-1}k_1\right] \\
\left(\beta c_{l_\theta}'\right)_{IV} &= \frac{8}{\pi}\left[\sqrt{my_1}\sqrt{1 - my_1} + m(\eta_1 - y_1)\tanh^{-1}k_1 + \right. \\
&\qquad \left. \tan^{-1}\sqrt{\frac{1 + m(\eta_1 - y_1)}{1 - m(\eta_1 - y_1)}} - \tan^{-1}\sqrt{\frac{1 - my_1}{my_1}}\right] \\
\left(\beta c_{l_\theta}'\right)_V &= \frac{8}{\pi}\left[\sqrt{my_1}\sqrt{m\eta_1} + m(\eta_1 - y_1)\tanh^{-1}k_2\right] \\
\left(\beta c_{l_\theta}'\right)_{VI} &= 0
\end{aligned}\right\} \qquad \text{(B9)}$$

and the particular form to use for $\beta c_{l_\theta}'$ is determined by the region in which the trailing edge falls.

The determination of $\beta c_{m_\theta}'$ requires evaluation of the integral of the potential along the chord of the wing. However, the indefinite integrals of the expressions for the potentials valid within each region happen to be continuous across the boundaries of each region. Furthermore, the indefinite integral of the potential that is valid in the neighborhood of the leading edge is zero at the leading edge. Thus, the integral of the potential along the chord may be found by evaluating at the trailing edge the indefinite integral of the potential that is valid within the region in which the trailing edge is located. When the trailing edge falls successively in each of the regions I to VI, the resulting equations for $\beta c_{m_\theta}'$ are, therefore,

$$\left.\begin{aligned}
\left(\beta c_{m_\theta}'\right)_{I} &= 0 \\
\left(\beta c_{m_\theta}'\right)_{II} &= \frac{8}{3\pi}(1 - my_1)^{3/2}\sqrt{my_1} \\
\left(\beta c_{m_\theta}'\right)_{III} &= \frac{4}{\pi} m(\eta_1 - y_1)\left[\tanh^{-1}k_1 - \frac{\sqrt{1 - m^2(\eta_1 - y_1)^2}}{2}\right] \\
\left(\beta c_{m_\theta}'\right)_{IV} &= \frac{4}{\pi}\left\{m(\eta_1 - y_1)\left[\tanh^{-1}k_1 - \frac{\sqrt{1 - m^2(\eta_1 - y_1)^2}}{2}\right] + \right. \\
&\qquad \left. \frac{2}{3}(1 - my_1)^{3/2}\sqrt{my_1}\right\} \\
\left(\beta c_{m_\theta}'\right)_{V} &= \frac{4}{\pi}\left[\left(1 - \frac{4m\eta_1}{3}\right)\sqrt{m\eta_1}\sqrt{my_1} + m(\eta_1 - y_1)\tanh^{-1}k_2\right] \\
\left(\beta c_{m_\theta}'\right)_{VI} &= 0
\end{aligned}\right\} \quad \text{(B10)}$$

where

$$k_1 = \sqrt{\frac{1 - m(\eta_1 - y_1)}{1 + m(\eta_1 - y_1)}} \qquad k_2 = \sqrt{\frac{y_1}{\eta_1}} \qquad \left(y_1 \leqq \eta_1\right)$$

$$k_1 = \sqrt{\frac{1 + m(\eta_1 - y_1)}{1 - m(\eta_1 - y_1)}} \qquad k_2 = \sqrt{\frac{\eta_1}{y_1}} \qquad \left(y_1 \geqq \eta_1\right)$$

As before, the particular form to use for $\beta c_{m_\theta}'$ is determined by the region in which the trailing edge falls.

Equations (B9) and (B10) may now be used to obtain the spanwise loading and twisting moment about the midchord due to a unit-step angle-of-attack distribution for particular values of η_1 and m. In summarizing the information, it is convenient to separate m and η_1 into various ranges. Sketches of the Mach lines and summaries of the particular forms to use in each range follow:

For $m \geqq 2$ and $0 \leqq \eta_1 \leqq \frac{1}{m}$:

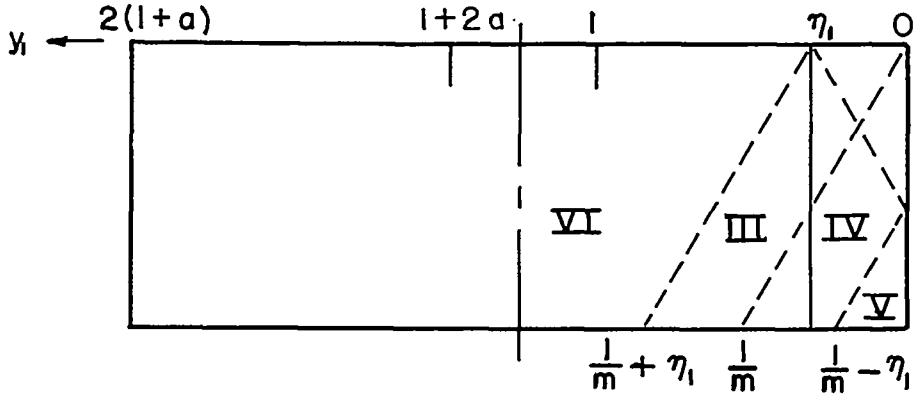

Use the coefficients

- for region V when $0 \leqq y_1 \leqq \frac{1}{m} - \eta_1$
- for region IV when $\frac{1}{m} - \eta_1 \leqq y_1 \leqq \frac{1}{m}$
- for region III when $\frac{1}{m} \leqq y_1 \leqq \frac{1}{m} + \eta_1$
- for region VI when $\frac{1}{m} + \eta_1 \leqq y_1 \leqq 2(1 + a)$

For $m \geqq 2$ and $\frac{1}{m} \leqq \eta_1 \leqq \frac{2}{m}$:

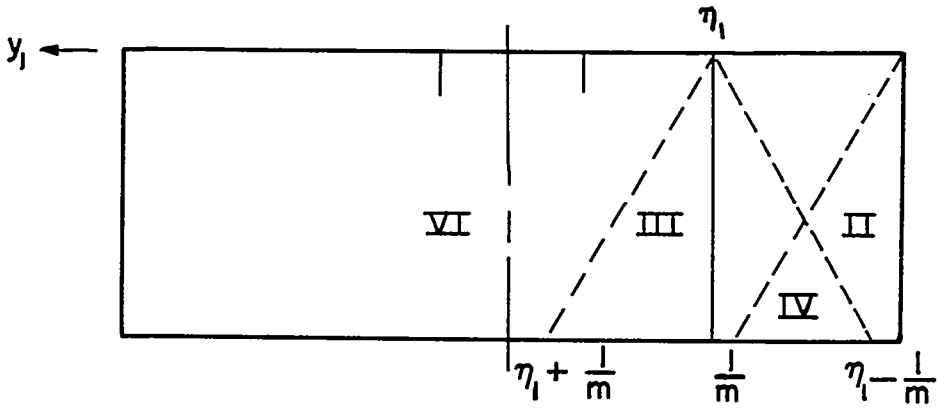

Use the coefficients

- for region II when $0 \leqq y_1 \leqq \eta_1 - \frac{1}{m}$
- for region IV when $\eta_1 - \frac{1}{m} \leqq y_1 \leqq \frac{1}{m}$
- for region III when $\frac{1}{m} \leqq y_1 \leqq \frac{1}{m} + \eta_1$
- for region VI when $\frac{1}{m} + \eta_1 \leqq y_1 \leqq 2(1 + a)$

For $m \geqq 2$ and $\frac{2}{m} \leqq \eta_1 \leqq 1$:

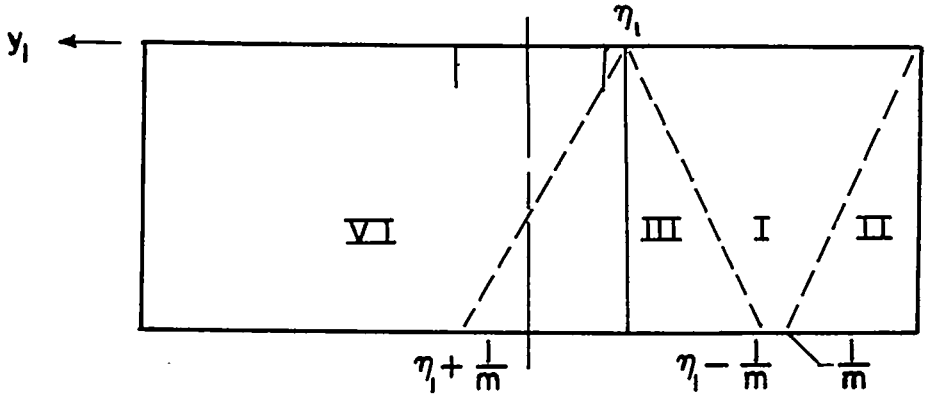

Use the coefficients
- for region II when $0 \leqq y_1 \leqq \frac{1}{m}$
- for region I when $\frac{1}{m} \leqq y_1 \leqq \eta_1 - \frac{1}{m}$
- for region III when $\eta_1 - \frac{1}{m} \leqq y_1 \leqq \eta_1 + \frac{1}{m}$
- for region VI when $\eta_1 + \frac{1}{m} \leqq y_1 \leqq 2(1 + a)$

For $\frac{1}{1 + 2a} \leqq m \leqq 2$ and $0 \leqq \eta_1 \leqq \frac{1}{m}$:

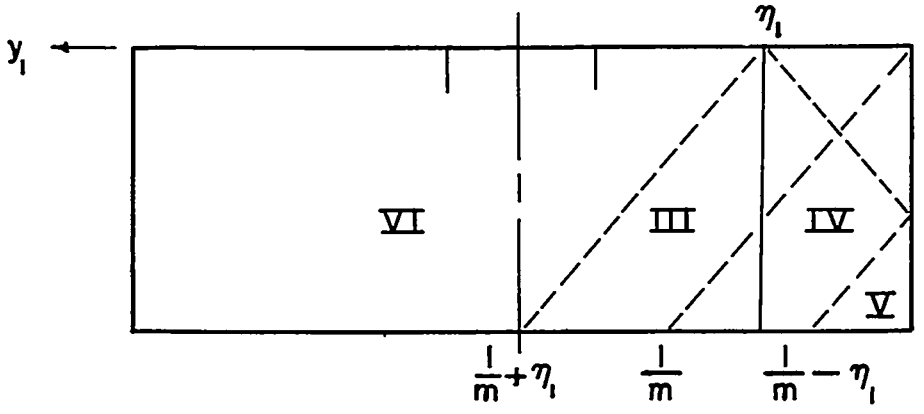

Use the coefficients
- for region V when $0 \leqq y_1 \leqq \frac{1}{m} - \eta_1$
- for region IV when $\frac{1}{m} - \eta_1 \leqq y_1 \leqq \frac{1}{m}$
- for region III when $\frac{1}{m} \leqq y_1 \leqq \frac{1}{m} + \eta_1$
- for region VI when $\frac{1}{m} + \eta_1 \leqq y_1 \leqq 2(1 + a)$

For $\frac{1}{1+2a} \leqq m \leqq 2$ and $\frac{1}{m} \leqq \eta_1 \leqq 1$:

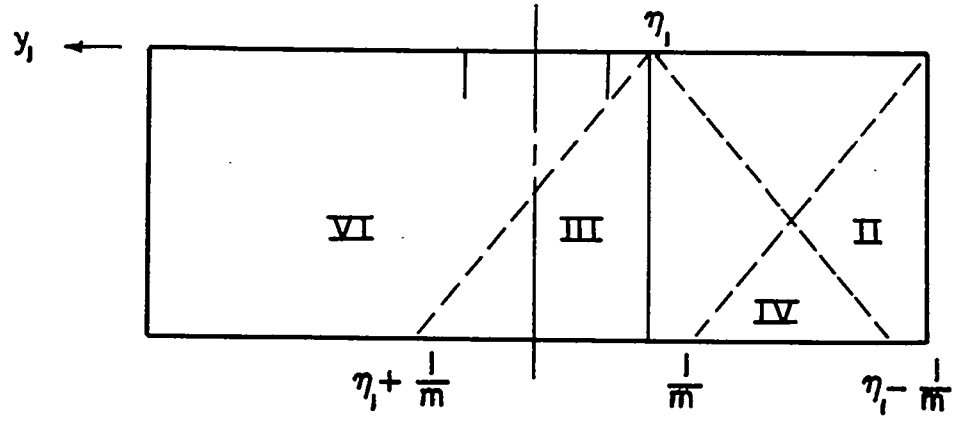

Use the coefficients

- for region II when $0 \leqq y_1 \leqq \eta_1 - \frac{1}{m}$
- for region IV when $\eta_1 - \frac{1}{m} \leqq y_1 \leqq \frac{1}{m}$
- for region III when $\frac{1}{m} \leqq y_1 \leqq \eta_1 + \frac{1}{m}$
- for region VI when $\eta_1 + \frac{1}{m} \leqq y_1 \leqq 2(1 + a)$

Derivation of βc_{l_p} and βc_{m_p}

The local angle of attack due to a unit rate of roll ($pb/2V = 1$) is given by

$$\sigma(\xi_1,\zeta_1) = -\left(1 - \frac{\zeta_1}{1+a}\right) \tag{B11}$$

The potential is therefore given by

$$\Phi(x_1,y_1) = -\iint_S \left(1 - \frac{\zeta_1}{1+a}\right) \frac{d\zeta_1\, d\xi_1}{\sqrt{(x_1 - \xi_1)^2 - m^2(y_1 - \zeta_1)^2}} \tag{B12}$$

In this section, the potential Φ is derived for a finite rectangular wing with a nondimensional span of $2(1 + a)$. In order to simplify the derivation, it is assumed that no point on the wing is influenced by both wing tips; this assumption is valid provided that $m \geqq \frac{1}{1 + a}$.

The Mach lines originating at the intersections of the leading edge and the tips divide the wing into two distinct regions (see the following sketches) and the potential Φ for these two regions is given by equation (B12) as follows:

In region I:

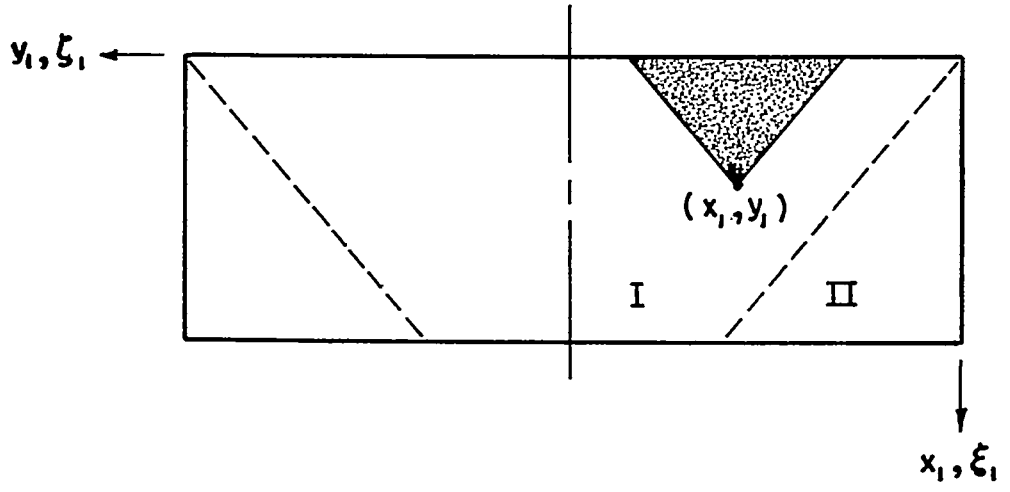

$$\Phi_I = -\frac{\pi}{m}\left(\frac{1 - y_1}{1 + a} + \frac{a}{1 + a}\right)$$

In region II:

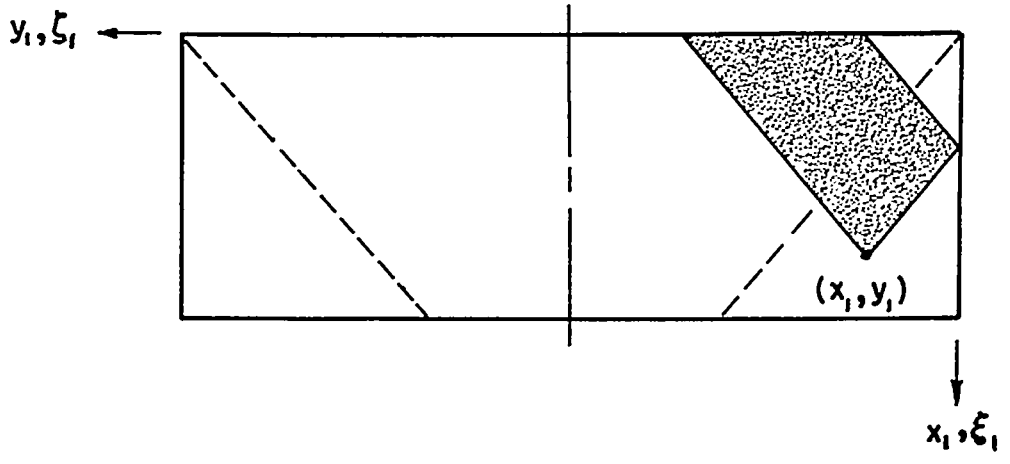

$$\Phi_{II} = -\frac{2}{m}\frac{1}{1+a}\left[\left(1 - \frac{y_1}{3} - \frac{2}{3}\frac{x_1}{m}\right)\sqrt{my_1}\sqrt{x_1 - my_1} + x_1(1 - y_1)\tan^{-1}\sqrt{\frac{my_1}{x_1 - my_1}}\right] -$$

$$\frac{2}{m}\frac{a}{1+a}\left(\sqrt{my_1}\sqrt{x_1 - my_1} + x_1 \tan^{-1}\sqrt{\frac{my_1}{x_1 - my_1}}\right)$$

The equations for the spanwise loading βc_{l_p} and the twisting moment about the midchord βc_{m_p} are found in a manner similar to that used to determine the equations for βc_{l_θ}' and βc_{m_θ}'. Thus,

$$\left.\begin{aligned}
\left(\beta c_{l_p}\right)_I &= -4\left(\frac{1 - y_1}{1 + a} + \frac{a}{1 + a}\right) \\
\left(\beta c_{l_p}\right)_{II} &= -\frac{8}{\pi}\frac{1}{1+a}\left[\left(1 - \frac{y_1}{3} - \frac{2}{3m}\right)\sqrt{my_1}\sqrt{1 - my_1} + \right. \\
&\qquad \left.(1 - y_1)\tan^{-1}\sqrt{\frac{my_1}{1 - my_1}}\right] - \frac{8}{\pi}\frac{a}{1+a}\left(\sqrt{my_1}\sqrt{1 - my_1} + \right. \\
&\qquad \left.\tan^{-1}\sqrt{\frac{my_1}{1 - my_1}}\right)
\end{aligned}\right\} \quad \text{(B13)}$$

The equations for βc_{m_p}, obtained in a manner similar to that used previously, are

$$\left.\begin{aligned}
\left(\beta c_{m_p}\right)_I &= 0 \\
\left(\beta c_{m_p}\right)_{II} &= -\frac{8}{\pi}\frac{1}{1+a}\left[\frac{1}{3}\left(1 - \frac{y_1}{5} + \frac{1}{5m}\right)\sqrt{my_1}\left(1 - my_1\right)^{3/2}\right] - \\
&\qquad \frac{8}{\pi}\frac{a}{1+a}\left[\frac{1}{3}\sqrt{my_1}(1 - my_1)^{3/2}\right]
\end{aligned}\right\} \quad \text{(B14)}$$

In order to conform to the assumption made in the aerodynamic analysis, the airloads over the rigid plate in the center section of the wing are to be neglected. Therefore, the limit of the modified aspect-ratio parameter can be lowered from $m \geqq \frac{1}{1+a}$ to $m \geqq \frac{1}{1+2a}$. Summaries of the particular forms to use and illustrative sketches follow:

For $m \geqq 1$:

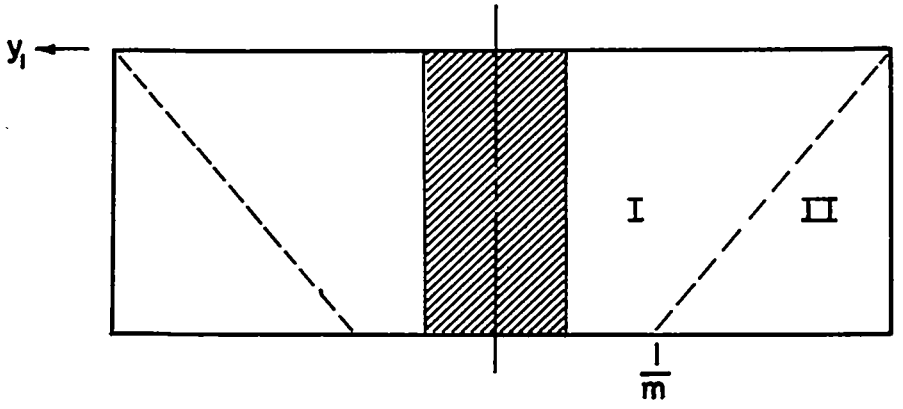

Use the coefficients
- for region II when $0 \leqq y_1 \leqq \frac{1}{m}$
- for region I when $\frac{1}{m} \leqq y_1 \leqq 1$

For $\frac{1}{1+2a} \leqq m \leqq 1$:

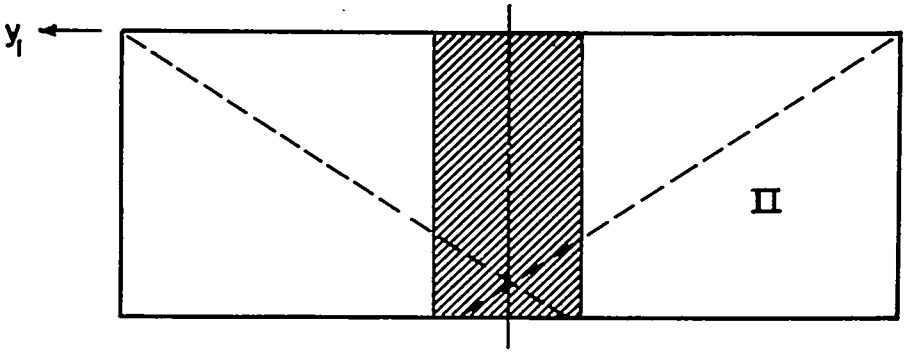

Use the coefficients for region II when $0 \leqq y_1 \leqq 1$

It should be noted that each expression for βc_{l_p} and βc_{m_p} can be separated into two parts - one with the coefficient $\frac{1}{1+a}$ and the other with the coefficient $\frac{a}{1+a}$ - each of which is independent of a. The first part is the result that would be obtained on the right wing if the wing were rolling about the x-axis (see fig. 2(a)); it is therefore designated $\beta c_{l_{p_o}}$ or $\beta c_{m_{p_o}}$. The second part can be shown to be the section lift or moment coefficient which results from a uniform angle of attack; it is therefore designated βc_{l_α} or βc_{m_α}. Thus, the quantities βc_{l_p} and βc_{m_p} can be written as

$$\beta c_{l_p} = \frac{1}{1+a}\beta c_{l_{p_o}} - \frac{a}{1+a}\beta c_{l_\alpha}$$

$$\beta c_{m_p} = \frac{1}{1+a}\beta c_{m_{p_o}} - \frac{a}{1+a}\beta c_{m_\alpha}$$

where the coefficients in the various regions are:

$$\left(\beta c_{l_{p_o}}\right)_I = -4(1 - y_1)$$

$$\left(\beta c_{l_\alpha}\right)_I = 4$$

$$\left(\beta c_{m_{p_o}}\right)_I = 0$$

$$\left(\beta c_{m_\alpha}\right)_I = 0$$

$$\left(\beta c_{l_{p_o}}\right)_{II} = -\frac{8}{\pi}\left[\left(1 - \frac{y_1}{3} - \frac{2}{3m}\right)\sqrt{my_1}\sqrt{1 - my_1} + (1 - y_1)\tan^{-1}\sqrt{\frac{my_1}{1 - my_1}}\right]$$

$$\left(\beta c_{l_\alpha}\right)_{II} = \frac{8}{\pi}\left(\sqrt{my_1}\sqrt{1 - my_1} + \tan^{-1}\sqrt{\frac{my_1}{1 - my_1}}\right)$$

$$\left(\beta c_{m_{p_o}}\right)_{II} = -\frac{8}{3\pi}\left(1 - \frac{y_1}{5} + \frac{1}{5m}\right)\sqrt{my_1}(1 - my_1)^{3/2}$$

$$\left(\beta c_{m_\alpha}\right)_{II} = \frac{8}{3\pi}\sqrt{my_1}(1 - my_1)^{3/2}$$

Derivation of βc_{l_δ} and βc_{m_δ}

In this section, the aerodynamic loads due to aileron deflection are derived for a trailing-edge aileron of constant chord c_a and span b_a. The spanwise location of the inboard end of the aileron is left general; the outboard end of the aileron coincides with the wing tip. It is assumed that there are no gaps between the aileron and the wing. Furthermore, the portion of the wing forward of the hinge line may be assumed to be absent because the wing is considered to be at zero angle of attack, the aileron hinge line is unswept, and only supersonic speeds are considered. The resulting configuration is exactly the same as that encountered in the derivation of βc_{l_θ} and βc_{m_θ}. In addition, since, for most reasonable aileron configurations, the pressures on the right wing are unaffected by the deflection of the left aileron, the total spanwise loading βc_{l_δ} and the total twisting moment about the midchord βc_{m_δ} can be found by properly substituting the aileron dimensions for the wing dimensions in the results already obtained for $\beta c_{l_\theta}'$ and $\beta c_{m_\theta}'$. In order that the foregoing be true, the restriction

$$m \geq \frac{c_{a_1}}{1 + 2a - b_{a_1}}$$ is necessary.

If c_a is substituted for c and $b_{a_1} = b_a/l$ for η_1 in the expressions for the loads due to structural deformation, the load due to a unit aileron deflection will result. Several more steps are necessary, however, in order to produce the desired results βc_{l_δ} and βc_{m_δ}. In the first place, the reduced aspect-ratio parameter which was $\beta l/c$ becomes $\beta l/c_a = m/c_{a_1}$, where $c_{a_1} = c_a/c$. In addition to the substitutions mentioned in the preceding paragraph, therefore, the substitution of m/c_{a_1} for m must be made, both in the expressions for $\beta c_{l_\theta}'$ and $\beta c_{m_\theta}'$ and in the expressions which define the limits of applicability of these terms. Furthermore, in the nondimensionalization of the moment expression the quantity c is involved. In order to preserve the nondimensionalizing coefficient qc/β for the aileron loads and qc^2/β for the aileron moments, the expressions for $\beta c_{l_\theta}'\left(y_1, b_{a_1}\right)$ and $\beta c_{m_\theta}'\left(y_1, b_{a_1}\right)$ must be multiplied by c_{a_1} and $c_{a_1}^2$, respectively. Lastly, since the moments are taken about the midchord in the case of pressures due to the structural deformation, direct substitution yields the moment about the aileron midchord; thus, the moment must be transferred back to the wing midchord.

The proper forms to use in determining βc_{l_δ} and βc_{m_δ} are summarized as follows for values of m greater than both $\frac{2c_{a_1}}{b_{a_1}}$ and $\frac{c_{a_1}}{1 + 2a - b_{a_1}}$:

For $b_{a_1} \leq 1 - \frac{c_{a_1}}{m}$:

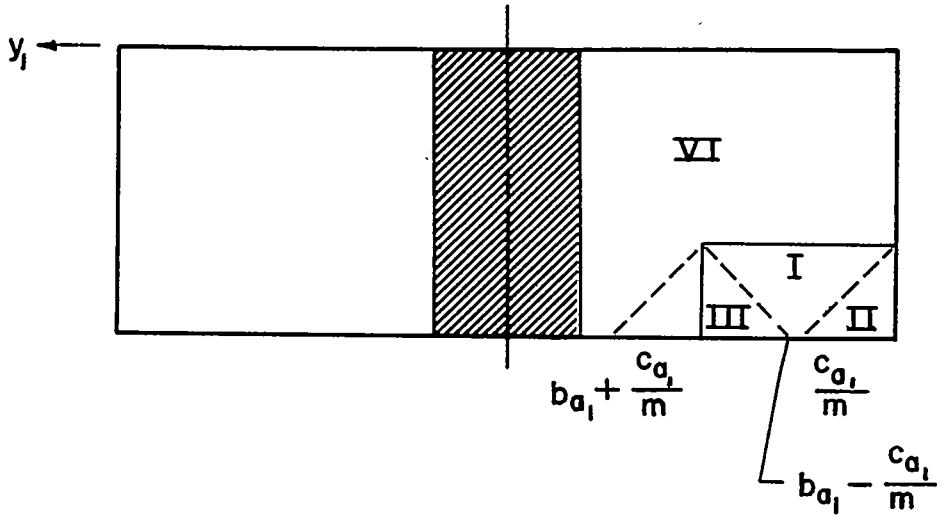

Use the coefficients

- for region II when $0 \leq y_1 \leq \frac{c_{a_1}}{m}$
- for region I when $\frac{c_{a_1}}{m} \leq y_1 \leq b_{a_1} - \frac{c_{a_1}}{m}$
- for region III when $b_{a_1} - \frac{c_{a_1}}{m} \leq y_1 \leq b_{a_1} + \frac{c_{a_1}}{m}$
- for region VI when $b_{a_1} + \frac{c_{a_1}}{m} \leq y_1 \leq 1$

For $b_{a_1} \geqq 1 - \frac{c_{a_1}}{m}$:

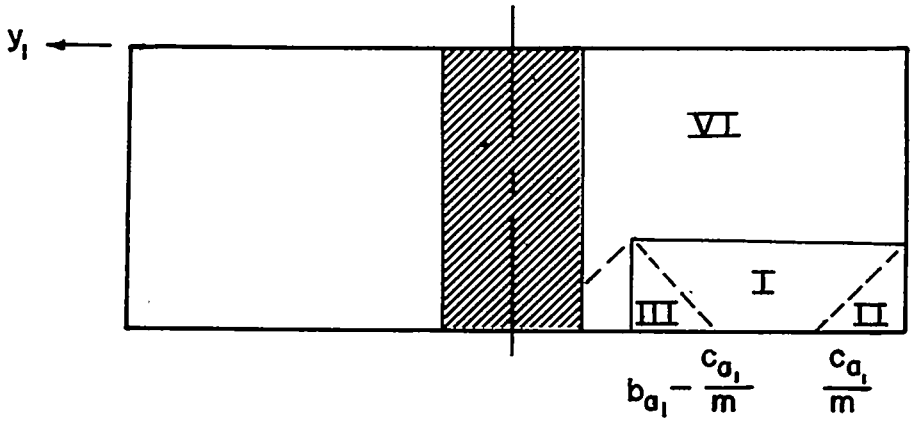

Use the coefficients
- for region II when $0 \leqq y_1 \leqq \frac{c_{a_1}}{m}$
- for region I when $\frac{c_{a_1}}{m} \leqq y_1 \leqq b_{a_1} - \frac{c_{a_1}}{m}$
- for region III when $b_{a_1} - \frac{c_{a_1}}{m} \leqq y_1 \leqq 1$

The expressions for the coefficients in the various ranges are:

$$\left(\beta c_{l_\delta}\right)_I = 4c_{a_1}$$

$$\left(\beta c_{l_\delta}\right)_{II} = \frac{8}{\pi}\left(\sqrt{my_1}\sqrt{c_{a_1} - my_1} + c_{a_1} \tan^{-1}\sqrt{\frac{my_1}{c_{a_1} - my_1}}\right)$$

$$\left(\beta c_{l_\delta}\right)_{III} = \frac{8}{\pi}\left[c_{a_1} \tan^{-1}\sqrt{\frac{c_{a_1} + m\left(b_{a_1} - y_1\right)}{c_{a_1} - m\left(b_{a_1} - y_1\right)}} + m\left(b_{a_1} - y_1\right)\tanh^{-1}k_1'\right]$$

$$\left(\beta c_{l_\delta}\right)_{VI} = 0$$

$$\left(\beta c_{m_\delta}\right)_I = -2c_{a_1}\left(1 - c_{a_1}\right)$$

$$\left(\beta c_{m_\delta}\right)_{II} = -\frac{4}{\pi}\left[\left(1 - \frac{5c_{a_1}}{3} + \frac{2my_1}{3}\right)\sqrt{my_1}\sqrt{c_{a_1} - my_1} + \left(1 - c_{a_1}\right)c_{a_1}\tan^{-1}\sqrt{\frac{my_1}{c_{a_1} - my_1}}\right]$$

$$\left(\beta c_{m_\delta}\right)_{III} = -\frac{4}{\pi}\left\{\left(1 - c_{a_1}\right)c_{a_1}\tan^{-1}\sqrt{\frac{c_{a_1} + m\left(b_{a_1} - y_1\right)}{c_{a_1} - m\left(b_{a_1} - y_1\right)}} + m\left(b_{a_1} - y_1\right)\left[\left(1 - 2c_{a_1}\right)\tanh^{-1}k_1' + \sqrt{\left(c_{a_1}\right)^2 - m^2\left(b_{a_1} - y_1\right)^2}\right]\right\}$$

$$\left(\beta c_{m_\delta}\right)_{VI} = 0$$

where

$$k_1' = \sqrt{\frac{c_{a_1} - m\left(b_{a_1} - y_1\right)}{c_{a_1} + m\left(b_{a_1} - y_1\right)}} \qquad \left(y_1 \leqq b_{a_1}\right)$$

$$k_1' = \sqrt{\frac{c_{a_1} + m\left(b_{a_1} - y_1\right)}{c_{a_1} - m\left(b_{a_1} - y_1\right)}} \qquad \left(y_1 \geqq b_{a_1}\right)$$

REFERENCES

1. Frick, C. W., and Chubb, R. S.: The Longitudinal Stability of Elastic Swept Wings at Supersonic Speed. NACA Rep. 965, 1950. (Supersedes NACA TN 1811.)

2. Schuerch, Hans U.: Structural Analysis of Swept, Low Aspect Ratio, Multispar Aircraft Wings. Aero. Eng. Rev., vol. 11, no. 11, Nov. 1952, pp. 34-41.

3. Levy, Samuel: Computation of Influence Coefficients for Aircraft Structures With Discontinuities and Sweepback. Jour. Aero. Sci., vol. 14, no. 10, Oct. 1947, pp. 547-560.

4. Reissner, Eric, and Stein, Manuel: Torsion and Transverse Bending of Cantilever Plates. NACA TN 2369, 1951.

5. The Staff of the Ames 1- by 3-Foot Supersonic Wind-Tunnel Section: Notes and Tables for Use in the Analysis of Supersonic Flow. NACA TN 1428, 1947.

6. Tucker, Warren A., and Nelson, Robert L.: The Flexible Rectangular Wing in Roll at Supersonic Flight Speeds. NACA TN 1769, 1948.

7. Stein, Manuel, Anderson, J. Edward, and Hedgepeth, John M.: Deflection and Stress Analysis of Thin Solid Wings of Arbitrary Plan Form With Particular Reference to Delta Wings. NACA Rep. 1131, 1953. (Supersedes NACA TN 2621.)

8. Lagerstrom, P. A., and Graham, Martha E.: Linearized Theory of Supersonic Control Surfaces. Jour. Aero. Sci., vol. 16, no. 1, Jan. 1949, pp. 31-34.

9. Harmon, Sidney M.: Stability Derivatives at Supersonic Speeds of Thin Rectangular Wings With Diagonals Ahead of Tip Mach Lines. NACA Rep. 925, 1949. (Supersedes NACA TN 1706.)

10. Evvard, John C.: Distribution of Wave Drag and Lift in the Vicinity of Wing Tips at Supersonic Speeds. NACA TN 1382, 1947.

TABLE I.- PARTIAL SECTION LIFT AND MOMENT COEFFICIENTS $\beta c_{l_\theta}'$ AND $\beta c_{m_\theta}'$

FOR A UNIT-STEP ANGLE OF ATTACK

(a) $\beta l/c = 5/7$

y/l	For η/l equal to -										
	0	0.1	0.2	0.3	0.4	0.5	0.6	0.7	0.8	0.9	1.0
	$\beta c_{l_\theta}'(y/l,\eta/l)$										
-1.3	0.023339	0	0	0	0	0	0	0	0	0	0
-1.2	.067298	.023339	0	0	0	0	0	0	0	0	0
-1.1	.126173	.067298	.023339	0	0	0	0	0	0	0	0
-1.0	.198493	.126173	.067298	.023339	0	0	0	0	0	0	0
-.9	.283854	.198493	.126173	.067298	.023339	0	0	0	0	0	0
-.8	.382447	.283854	.198493	.126173	.067298	.023339	0	0	0	0	0
-.7	.494931	.382447	.283854	.198493	.126173	.067298	.023339	0	0	0	0
-.6	.622469	.494931	.382447	.283854	.198493	.126173	.067298	.023339	0	0	0
-.5	.755859	.622469	.494931	.382447	.283854	.198493	.126173	.067298	.023339	0	0
-.4	.930849	.766859	.622469	.494931	.382447	.283854	.198493	.126173	.067298	.023339	0
-.3	1.04930	.897717	.733726	.589337	.461799	.349315	.250723	.165362	.093041	.034167	0
-.2	1.24247	1.022886	.854923	.670937	.526543	.399010	.286521	.187932	.102572	.035611	0
-.1	1.42537	1.157726	.938137	.750178	.586189	.441798	.314260	.201778	.107498	.037253	0
0	1.71432	1.320358	1.052711	.833126	.645163	.481175	.336785	.213062	.113216	.039149	0
.1	1.98315	1.589087	1.195130	.927484	.707896	.519936	.359491	.226504	.119961	.041365	0
.2	2.10430	1.836762	1.442695	1.048740	.781092	.564900	.387676	.242903	.128081	.044005	0
.3	2.15443	1.934844	1.667305	1.273240	.882613	.625377	.424091	.263557	.138125	.047229	0
.4	2.14681	1.958854	1.739267	1.474968	1.091348	.715331	.474109	.290757	.151004	.051285	0
.5	2.08438	1.920391	1.735864	1.526792	1.277190	.909457	.550858	.329142	.168392	.056609	0
.6	1.96398	1.823206	1.670192	1.500869	1.308059	1.076031	.727565	.390548	.193838	.064041	0
.7	1.77946	1.663767	1.539261	1.403506	1.252644	1.079785	.869634	.545674	.237054	.075502	0
.8	1.51367	1.423440	1.327050	1.223027	1.109179	.981991	.835096	.654029	.363783	.096919	0
.9	1.11123	1.049983	.984929	.915250	.839798	.756835	.663525	.554592	.417548	.181891	0
1.0	0	0	0	0	0	0	0	0	0	0	0
	$\beta c_{m_\theta}'(y/l,\eta/l)$										
-1.3	-0.010999	0	0	0	0	0	0	0	0	0	0
-1.2	-.029761	-.010999	0	0	0	0	0	0	0	0	0
-1.1	-.052085	-.029761	-.010999	0	0	0	0	0	0	0	0
-1.0	-.076012	-.052085	-.029764	-.010999	0	0	0	0	0	0	0
-.9	-.100087	-.076012	-.052085	-.029761	-.010999	0	0	0	0	0	0
-.8	-.123018	-.100087	-.076012	-.052085	-.029761	-.010999	0	0	0	0	0
-.7	-.143537	-.123018	-.100087	-.076012	-.052085	-.029761	-.010999	0	0	0	0
-.6	-.160289	-.143537	-.123018	-.100087	-.076012	-.052085	-.029761	-.010999	0	0	0
-.5	-.171703	-.160289	-.143537	-.123018	-.100087	-.076012	-.052085	-.029761	-.010999	0	0
-.4	-.175804	-.171703	-.160289	-.143537	-.123018	-.100087	-.076012	-.052085	-.029761	-.010999	0
-.3	-.154246	-.160190	-.156087	-.144674	-.127922	-.107401	-.084472	-.060397	-.036470	-.014145	0
-.2	-.107098	-.127428	-.133372	-.129270	-.117857	-.101104	-.080584	-.057654	-.033579	-.012198	0
-.1	-.031475	-.074895	-.095225	-.101170	-.097067	-.085653	-.068902	-.048381	-.027503	-.010100	0
0	.109560	.003450	-.039971	-.060299	-.066244	-.062141	-.050727	-.035792	-.020862	-.007815	0
.1	.251367	.145258	.039147	-.004272	-.024602	-.030546	-.028130	-.021767	-.013514	-.005301	0
.2	.329556	.286136	.180025	.073915	.030495	.008549	.002149	.005845	.005251	.002495	0
.3	.382066	.361737	.318317	.212207	.104509	.055480	.028715	.012702	.004245	.000698	0
.4	.415838	.409894	.389565	.344554	.233860	.120461	.067324	.035135	.015493	.004426	0
.5	.433166	.437268	.429691	.404701	.353949	.238191	.120487	.063932	.029415	.008936	0
.6	.434189	.443882	.443121	.429608	.399434	.344338	.225199	.105261	.047922	.014697	0
.7	.415320	.426825	.430171	.423910	.405836	.372163	.314800	.194884	.076094	.022748	0
.8	.369481	.380991	.386357	.384655	.374563	.354045	.319554	.263366	.147246	.036210	0
.9	.281716	.291131	.296477	.297212	.292601	.281579	.262471	.232288	.184276	.082284	0
1.0	0	0	0	0	0	0	0	0	0	0	0

TABLE I.- PARTIAL SECTION LIFT AND MOMENT COEFFICIENTS $\beta c_{l_\theta}'$ AND $\beta c_{m_\theta}'$

FOR A UNIT-STEP ANGLE OF ATTACK - Continued

(b) $\beta l/c = 1$

y/l	For η/l equal to -										
	0	0.1	0.2	0.3	0.4	0.5	0.6	0.7	0.8	0.9	1.0
	$\beta c_{l_\theta}'(y/l,\eta/l)$										
-0.9	0.038956	0	0	0	0	0	0	0	0	0	0
-.8	.113297	.038956	0	0	0	0	0	0	0	0	0
-.7	.214524	.113297	.038956	0	0	0	0	0	0	0	0
-.6	.341391	.214524	.113297	.038956	0	0	0	0	0	0	0
-.5	.494934	.341391	.214524	.113297	.038956	0	0	0	0	0	0
-.4	.678079	.494934	.341391	.214524	.113297	.038956	0	0	0	0	0
-.3	.896307	.678079	.494934	.341391	.214524	.113297	.038956	0	0	0	0
-.2	1.159858	.896307	.678079	.494934	.341391	.214524	.113297	.038956	0	0	0
-.1	1.491353	1.159858	.896307	.678079	.494934	.341391	.214524	.113297	.038956	0	0
0	2.000000	1.491351	1.159860	.896307	.678076	.494934	.341389	.214524	.113298	.038956	0
.1	2.453263	1.944614	1.435965	1.104472	.840921	.622691	.439545	.286005	.159137	.057904	0
.2	2.678063	2.346570	1.837924	1.329272	.997784	.734229	.516001	.332855	.179313	.061607	0
.3	2.794595	2.531045	2.199552	1.690903	1.182254	.850761	.587210	.368980	.193375	.066116	0
.4	2.825815	2.607584	2.344034	2.012541	1.503895	.995243	.663753	.407062	.211406	.071799	0
.5	2.778311	2.595163	2.376932	2.113382	1.781889	1.273240	.771201	.460798	.235749	.079250	0
.6	2.649749	2.496209	2.313084	2.094850	1.851283	1.506444	1.018592	.546767	.271373	.089656	0
.7	2.428463	2.301597	2.148057	1.964909	1.753704	1.511699	1.217489	.763944	.331875	.105701	0
.8	2.085961	1.984736	1.857870	1.712237	1.552851	1.374788	1.169134	.915640	.509296	.135688	0
.9	1.544320	1.469978	1.378901	1.281350	1.175722	1.059575	.928935	.776427	.584570	.254648	0
1.0	0	0	0	0	0	0	0	0	0	0	0
	$\beta c_{m_\theta}'(y/l,\eta/l)$										
-0.9	-0.017908	0	0	0	0	0	0	0	0	0	0
-.8	-.047438	-.017808	0	0	0	0	0	0	0	0	0
-.7	-.080858	-.047438	-.017908	0	0	0	0	0	0	0	0
-.6	-.114061	-.080858	-.047438	-.017908	0	0	0	0	0	0	0
-.5	-.143536	-.114061	-.080858	-.047438	-.017908	0	0	0	0	0	0
-.4	-.165594	-.143536	-.114061	-.080858	-.047438	-.017908	0	0	0	0	0
-.3	-.175684	-.165594	-.143536	-.114061	-.080858	-.047438	-.017908	0	0	0	0
-.2	-.167131	-.175684	-.165594	-.143536	-.114061	-.080858	-.047438	-.017908	0	0	0
-.1	-.127212	-.167131	-.175684	-.165594	-.143536	-.114061	-.080858	-.047438	-.017908	0	0
0	0	-.127212	-.167131	-.175684	-.165594	-.143536	-.114062	-.080858	-.047438	-.017908	0
.1	-.152677	.025464	-.101748	-.141666	-.150219	-.140129	-.118071	-.088596	-.055393	-.021977	0
.2	.255037	.195119	.067905	-.059306	-.099224	-.107778	-.097688	-.075629	-.046156	-.017213	0
.3	.292379	.283825	.243907	.116694	-.010518	-.050436	-.058989	-.048899	-.030353	-.011857	0
.4	.331928	.342019	.333467	.293547	.166336	.039122	-.000794	-.012545	-.011913	-.005684	0
.5	.355743	.377801	.387891	.379338	.339419	.212207	.081914	.033149	.010505	.001664	0
.6	.363565	.393039	.415098	.425187	.416635	.373614	.237672	.096958	.039652	.010873	0
.7	.353146	.386348	.415823	.437881	.444699	.427101	.373510	.229183	.082769	.023446	0
.8	.319064	.352484	.385686	.411475	.423574	.418971	.392499	.333068	.186742	.043835	0
.9	.247091	.276623	.305315	.326265	.338357	.339983	.328655	.300000	.244267	.110347	
1.0	0	0	0	0	0	0	0	0	0	0	0

TABLE I.- PARTIAL SECTION LIFT AND MOMENT COEFFICIENTS $\beta c_{l_\theta}'$ AND $\beta c_{m_\theta}'$

FOR A UNIT-STEP ANGLE OF ATTACK - Continued

(c) $\beta l/c = 4/3$

y/l	For η/l equal to -										
	0	0.1	0.2	0.3	0.4	0.5	0.6	0.7	0.8	0.9	1.0
	$\beta c_{l_\theta}'(y/l,\eta/l)$										
-0.7	0.021016	0	0	0	0	0	0	0	0	0	0
-.6	.113298	.021016	0	0	0	0	0	0	0	0	0
-.5	.253952	.113298	.021016	0	0	0	0	0	0	0	0
-.4	.440646	.253952	.113298	.021016	0	0	0	0	0	0	0
-.3	.678076	.440646	.253952	.113298	.021016	0	0	0	0	0	0
-.2	.978405	.678076	.440646	.253952	.113298	.021016	0	0	0	0	0
-.1	1.370753	.978405	.678076	.440646	.253952	.113298	.021016	0	0	0	0
0	2.000000	1.370753	.978405	.678076	.440646	.253952	.113298	.021016	0	0	0
.1	2.629246	2.000000	1.370753	.978405	.678076	.440646	.253952	.113298	.021016	0	0
.2	3.021605	2.629246	2.000000	1.370753	.978395	.678076	.440646	.253952	.113298	.021016	0
.3	3.292095	2.991777	2.599419	1.970174	1.340925	.948567	.648249	.410818	.224124	.083470	0
.4	3.397278	3.159848	2.859530	2.467172	1.837926	1.208678	.816320	.516002	.278571	.095730	0
.5	3.379164	3.192470	2.955040	2.654721	2.262363	1.633118	1.003870	.611522	.314331	.105669	0
.6	3.242058	3.101401	2.914707	2.677276	2.376958	1.984600	1.355355	.729023	.361831	.119542	0
.7	2.970118	2.877841	2.737187	2.550492	2.313062	2.012737	1.623319	1.018592	.442500	.140936	
.8	2.507915	2.507915	2.394621	2.253963	2.067269	1.833051	1.558846	1.220853	.679061	.180917	0
.9	1.817493	1.817493	1.817493	1.704192	1.567623	1.412759	1.238580	1.035232	.779423	.339531	0
1.0	0	0	0	0	0	0	0	0	0	0	0
	$\beta c_{m_\theta}'(y/l,\eta/l)$										
-0.7	-0.009946	0	0	0	0	0	0	0	0	0	0
-.6	-.047439	-.009946	0	0	0	0	0	0	0	0	0
-.5	-.092126	-.047439	-.009946	0	0	0	0	0	0	0	0
-.4	-.134344	-.092126	-.047439	-.009946	0	0	0	0	0	0	0
-.3	-.165594	-.134344	-.092126	-.047439	-.009946	0	0	0	0	0	0
-.2	-.175340	-.165594	-.134344	-.092126	-.047439	-.009946	0	0	0	0	0
-.1	-.145363	-.175340	-.165594	-.134344	-.092126	-.047439	-.009946	0	0	0	0
.0	0	-.145363	-.175340	-.165594	-.134344	-.092126	-.047439	-.009946	0	0	0
.1	.145363	0	-.145363	-.175340	-.165594	-.134344	-.092126	-.047439	-.009946	0	0
.2	.175340	.145363	0	-.145363	-.175340	-.165594	-.134344	-.092126	-.047439	-.009946	0
.3	.179710	.189456	.159479	.141157	-.131247	-.161224	-.151478	-.120229	-.078010	-.033323	0
.4	.202250	.233500	.243246	.213269	.067906	-.077456	-.107343	-.097687	-.066437	-.026062	0
.5	.225508	.267723	.298974	.308722	.278743	.133380	.011982	-.041960	-.033713	-.014650	0
.6	.245058	.289745	.331962	.363213	.372959	.342982	.197619	.050866	.010187	-.000590	0
.7	.259451	.296943	.341631	.383848	.415098	.424844	.393465	.237671	.073396	.018193	0
.8	.275268	.275268	.322707	.367394	.409611	.439329	.437969	.388647	.218809	.047776	0
.9	.250073	.250073	.250073	.297512	.340250	.368951	.377847	.360794	.304348	.139585	0
1.0	0	0	0	0	0	0	0	0	0	0	0

TABLE I.- PARTIAL SECTION LIFT AND MOMENT COEFFICIENTS $\beta c_{l_\theta}'$ AND $\beta c_{m_\theta}'$

FOR A UNIT-STEP ANGLE OF ATTACK - Continued

(d) $\beta l/c = 2$

y/l	For η/l equal to -										
	0	0.1	0.2	0.3	0.4	0.5	0.6	0.7	0.8	0.9	1.0
	$\beta c_{l_\theta}'(y/l, \eta/l)$										
-0.4	0.113298	0	0	0	0	0	0	0	0	0	0
-.3	.341391	.113298	0	0	0	0	0	0	0	0	0
-.2	.678076	.341391	.113298	0	0	0	0	0	0	0	0
-.1	1.159860	.678076	.341391	.113298	0	0	0	0	0	0	0
0	2.000000	1.159860	.678076	.341391	.113298	0	0	0	0	0	0
.1	2.840139	2.000000	1.159860	.678076	.341391	.113298	0	0	0	0	0
.2	3.321923	2.840139	2.000000	1.159860	.678076	.341391	.113298	0	0	0	0
.3	3.658608	3.321923	2.840139	2.000000	1.159860	.678076	.341391	.113298	0	0	0
.4	3.886701	3.658608	3.321923	2.840139	2.000000	1.159860	.678076	.341391	.113298	0	0
.5	4.000000	3.886701	3.658608	3.321923	2.840139	2.000000	1.159860	.678076	.341391	.113298	0
.6	3.387921	3.837921	3.724623	3.496530	3.159844	2.678061	1.837921	.997782	.515998	.179313	0
.7	3.503889	3.503889	3.503889	3.390596	3.162503	2.825813	2.344029	1.503889	.663755	.211409	0
.8	2.991140	2.991140	2.991140	2.991140	2.877837	2.649749	2.313059	1.831270	1.018592	.271373	0
.9	2.199262	2.199262	2.199262	2.199262	2.199262	2.085964	1.857870	1.552848	1.169134	.509296	0
1.0	0	0	0	0	0	0	0	0	0	0	0
	$\beta c_{m_\theta}'(y/l, \eta/l)$										
-0.4	-0.047438	0	0	0	0	0	0	0	0	0	0
-.3	-.114062	-.047438	0	0	0	0	0	0	0	0	0
-.2	-.165592	-.114062	-.047438	0	0	0	0	0	0	0	0
-.1	-.167131	-.165592	-.114062	-.047438	0	0	0	0	0	0	0
0	0	-.167131	-.165595	-.114062	-.047438	0	0	0	0	0	0
.1	.167131	0	-.167131	-.165592	-.114062	-.047438	0	0	0	0	0
.2	.165595	.167131	0	-.167131	-.165565	-.114062	-.047438	0	0	0	0
.3	.114062	.165592	.167131	0	-.167131	-.165592	-.114062	-.047438	0	0	0
.4	.047438	.114062	.165595	.167131	0	-.167131	-.165595	-.114062	-.047438	0	0
.5	0	.047438	.114062	.165592	.167131	0	-.167131	-.165592	-.114062	-.047438	0
.6	.067907	.067907	.115345	.181969	.233502	.235035	.067907	-.099223	-.097688	-.046154	0
.7	.166336	.166336	.166336	.213774	.280398	.331928	.333467	.166336	-.000793	-.011912	0
.8	.249504	.249504	.249504	.249504	.296942	.363566	.415099	.416632	.237672	.039653	0
.9	.271625	.271625	.271625	.271625	.271625	.319064	.385685	.423574	.392499	.186741	0
1.0	0	0	0	0	0	0	0	0	0	0	0

TABLE I.- PARTIAL SECTION LIFT AND MOMENT COEFFICIENTS $\beta c_{l_\theta}'$ AND $\beta c_{m_\theta}'$

FOR A UNIT-STEP ANGLE OF ATTACK - Concluded

(e) $\beta l/c = 4$

y/l	For η/l equal to -										
	0	0.1	0.2	0.3	0.4	0.5	0.6	0.7	0.8	0.9	1.0
	$\beta c_{l_\theta}'(y/l,\eta/l)$										
-0.2	0.113298	0	0	0	0	0	0	0	0	0	0
-.1	.678075	.113298	0	0	0	0	0	0	0	0	0
0	2.000000	.678075	.113298	0	0	0	0	0	0	0	0
.1	3.321923	2.000000	.678075	.113298	0	0	0	0	0	0	0
.2	3.886711	3.321923	2.000000	.678075	.113298	0	0	0	0	0	0
.3	4.000000	3.886701	3.321923	2.000000	.678076	.113298	0	0	0	0	0
.4	4.000000	4.000000	3.886711	3.321923	2.000000	.678075	.113298	0	0	0	0
.5	4.000000	4.000000	4.000000	3.886701	3.321923	2.000000	.678076	.113298	0	0	0
.6	4.000000	4.000000	4.000000	4.000000	3.886711	3.321923	2.000000	.678075	.113298	0	0
.7	4.000000	4.000000	4.000000	4.000000	4.000000	3.886701	3.321923	2.000000	.678076	.113298	0
.8	3.837920	3.837920	3.837920	3.837920	3.837920	3.837900	3.724633	3.159844	1.837926	.515998	0
.9	2.991145	2.991145	2.991145	2.991145	2.991145	2.991145	2.991145	2.877837	2.313059	1.018592	0
1.0	0	0	0	0	0	0	0	0	0	0	0
	$\beta c_{m_\theta}'(y/l,\eta/l)$										
-0.2	-0.047438	0	0	0	0	0	0	0	0	0	0
-.1	-.165594	-.047438	0	0	0	0	0	0	0	0	0
0	0	-.165594	-.047438	0	0	0	0	0	0	0	0
.1	.165594	0	.165594	-.047438	0	0	0	0	0	0	0
.2	.047438	.165594	0	-.165594	-.047438	0	0	0	0	0	0
.3	0	.047438	.165594	0	-.165594	-.047438	0	0	0	0	0
.4	0	0	.047438	.165594	0	-.165594	-.047438	0	0	0	0
.5	0	0	0	.047438	.165594	0	-.165594	-.047438	0	0	0
.6	0	0	0	0	.047438	.165594	0	-.165594	-.047438	0	0
.7	0	0	0	0	0	.047438	.165594	0	-.165594	-.047438	0
.8	.679044	.067904	.067904	.067904	.067904	.067904	.115356	.233502	.067905	-.097688	0
.9	.249504	.259504	.249504	.249504	.249504	.249504	.249504	.296940	.414640	.237672	0
1.0	0	0	0	0	0	0	0	0	0	0	0

TABLE II.- SECTION LIFT AND MOMENT COEFFICIENTS βc_{l_p} AND βc_{m_p}

FOR A UNIT RATE OF ROLL

$$\left[\begin{aligned} \beta c_{l_p} &= -\frac{a}{1+a}\,\beta c_{l_\alpha} + \frac{1}{1+a}\,\beta c_{l_{p_o}} \\ \beta c_{m_p} &\doteq -\frac{a}{1+a}\,\beta c_{m_\alpha} + \frac{1}{1+a}\,\beta c_{m_{p_o}} \end{aligned}\right]$$

y/l	$\beta c_{l_\alpha}(y/l)$	$\beta c_{l_{p_o}}(y/l)$	$\beta c_{m_\alpha}(y/l)$	$\beta c_{m_{p_o}}(y/l)$
		(a) $\beta l/c = 5/7$		
0	3.714314	0.306768	0.109560	-0.118325
.1	3.589100	.047812	.145258	-.159784
.2	3.442694	-.184467	.180026	-.201629
.3	3.273239	-.387793	.212207	-.241915
.4	3.077662	-.558969	.240010	-.278412
.5	2.851240	-.693521	.261463	-.308527
.6	2.586448	-.784948	.273900	-.328680
.7	2.270441	-.823060	.273661	-.333866
.8	1.878086	-.789604	.254594	-.315697
.9	1.344769	-.641916	.202991	-.255769
1.0	0	0	0	0
		(b) $\beta l/c = 1$		
0	4.000000	0	0	0
.1	3.944613	-.343532	.025464	-.025974
.2	3.837918	-.631772	.067905	-.070621
.3	3.690902	-.873882	.116694	-.123696
.4	3.503889	-1.068886	.166334	-.179641
.5	3.273240	-1.212206	.212207	-.233427
.6	2.991135	-1.295676	.249503	-.279443
.7	2.642985	-1.305516	.272287	-.310407
.8	2.199256	-1.216158	.271624	-.315084
.9	1.583274	-.966580	.229183	-.270436
1.0	0	0	0	0
		(c) $\beta l/c = 4/3$		
0	4.000000	0	0	0
.1	4.000000	-.400000	0	0
.2	4.000000	-.800000	0	0
.3	3.970171	-1.169877	.014115	-.014256
.4	3.837919	-1.433309	.067906	-.069943
.5	3.633116	-1.616485	.133380	-.140049
.6	3.355351	-1.716783	.197619	-.211452
.7	2.991142	-1.719543	.249502	-.271957
.8	2.507913	-1.593429	.275267	-.305547
.9	1.817491	-1.260633	.250073	-.282582
1.0	0	0	0	0

TABLE II.- SECTION LIFT AND MOMENT COEFFICIENTS βc_{l_p} AND βc_{m_p}

FOR A UNIT RATE OF ROLL - Concluded

$$\left[\begin{aligned} \beta c_{l_p} &= -\frac{a}{1+a}\,\beta c_{l_\alpha} + \frac{1}{1+a}\,\beta c_{l_{p_o}} \\ \beta c_{m_p} &= -\frac{a}{1+a}\,\beta c_{m_\alpha} + \frac{1}{1+a}\,\beta c_{m_{p_o}} \end{aligned}\right]$$

y/l	$\beta c_{l_\alpha}(y/l)$	$\beta c_{l_{p_o}}(y/l)$	$\beta c_{m_\alpha}(y/l)$	$\beta c_{m_{p_o}}(y/l)$
(d) $\beta l/c = 2$				
0	4.000000	0	0	0
.1	4.000000	-.400000	0	0
.2	4.000000	-.800000	0	0
.3	4.000000	-1.200000	0	0
.4	4.000000	-1.600000	0	0
.5	4.000000	-2.000000	0	0
.6	3.837921	-2.234846	.067906	-.069264
.7	3.503723	-2.286270	.166336	-.172989
.8	2.991137	-2.143407	.249504	-.264474
.9	2.199274	-1.707722	.271624	-.293354
1.0	0	0	0	0
(e) $\beta l/c = 4$				
0	4.000000	0	0	0
.1	4.000000	-.400000	0	0
.2	4.000000	-.800000	0	0
.3	4.000000	-1.200000	0	0
.4	4.000000	-1.600000	0	0
.5	4.000000	-2.000000	0	0
.6	4.000000	-2.400000	0	0
.7	4.000000	-2.800000	0	0
.8	3.837920	-3.036384	.067906	-.068585
.9	2.991135	-2.567274	.249503	-.256987
1.0	0	0	0	0

TABLE III.- SECTIONAL LIFT AND MOMENT COEFFICIENTS βc_{l_δ} AND βc_{m_δ}

FOR A UNIT AILERON DEFLECTION

$$\begin{bmatrix} a \geqq 0.14 \\ b_a/l = 1.0 \\ c_a/c = 0.2 \end{bmatrix}$$

y/l	$\beta c_{l_\delta}(y/l)$	$\beta c_{m_\delta}(y/l)$
(a) $\beta l/c = 5/7$		
0	-0.400000	-0.160000
.1	-.646627	-.251783
.2	-.760302	-.301080
.3	-.800000	-.320000
.4	-.800000	-.320000
.5	-.800000	-.320000
.6	-.800000	-.320000
.7	-.800000	-.320000
.8	-.742863	-.292771
.9	-.570248	-.217640
1.0	0	0
(b) $\beta l/c = 1$		
0	-0.400000	-0.160000
.1	-.701015	-.274665
.2	-.800000	-.320000
.3	-.800000	-.320000
.4	-.800000	-.320000
.5	-.800000	-.320000
.6	-.800000	-.320000
.7	-.800000	-.320000
.8	-.800000	-.320000
.9	-.654649	-.253370
1.0	0	0

y/l	$\beta c_{l_\delta}(y/l)$	$\beta c_{m_\delta}(y/l)$
(c) $\beta l/c = 4/3$		
0	-0.400000	-0.160000
.1	-.749212	-.295998
.2	-.800000	-.320000
.3	-.800000	-.320000
.4	-.800000	-.320000
.5	-.800000	-.320000
.6	-.800000	-.320000
.7	-.800000	-.320000
.8	-.800000	-.320000
.9	-.726623	-.285314
1.0	0	0
(d) $\beta l/c \geqq 2$		
0	-0.400000	-0.160000
.1	-.800000	-.320000
.2	-.800000	-.320000
.3	-.800000	-.320000
.4	-.800000	-.320000
.5	-.800000	-.320000
.6	-.800000	-.320000
.7	-.800000	-.320000
.8	-.800000	-.320000
.9	-.800000	-.320000
1.0	0	0

TABLE IV.- INFLUENCE COEFFICIENT MATRIX $\left[\frac{\partial G_M}{\partial y}\right]$

USED IN SAMPLE CALCULATIONS

$$\left[\frac{\partial G_M}{\partial y}\right] = \frac{1}{\frac{Gt^3c}{3}} \begin{bmatrix} 0 & 0 & 0 & 0 & 0 & 0 & 0 & 0 & 0 & 0 & 0 \\ 0 & 0.055872 & 0.244188 & 0.449316 & 0.561924 & 0.623772 & 0.657864 & 0.676728 & 0.687456 & 0.693972 & 0.698760 \\ 0 & 0.016848 & 0.073584 & 0.191304 & 0.413712 & 0.638496 & 0.761040 & 0.829440 & 0.868248 & 0.891900 & 0.909180 \\ 0 & 0.005112 & 0.022320 & 0.058068 & 0.125532 & 0.249804 & 0.476928 & 0.705708 & 0.835560 & 0.914688 & 0.972396 \\ 0 & 0.001656 & 0.007272 & 0.018900 & 0.040896 & 0.081396 & 0.155412 & 0.290376 & 0.536400 & 0.799236 & 0.991008 \\ 0 & 0.000936 & 0.004032 & 0.010440 & 0.022608 & 0.044964 & 0.085824 & 0.160380 & 0.296244 & 0.543816 & 0.995040 \end{bmatrix}$$

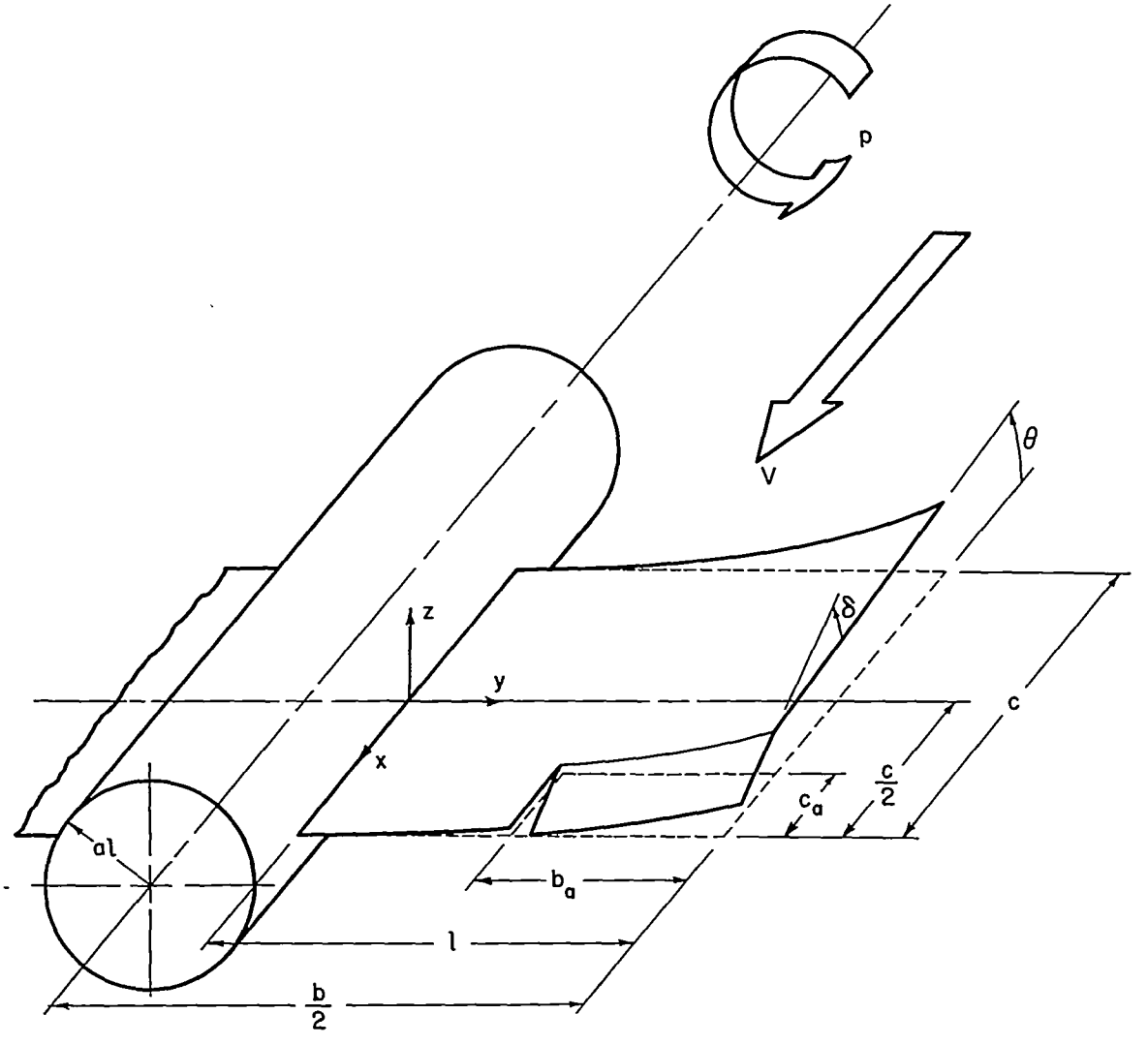

Figure 1.- Configuration considered in the aeroelastic analysis. Positive directions of displacements and velocities are indicated by arrows.

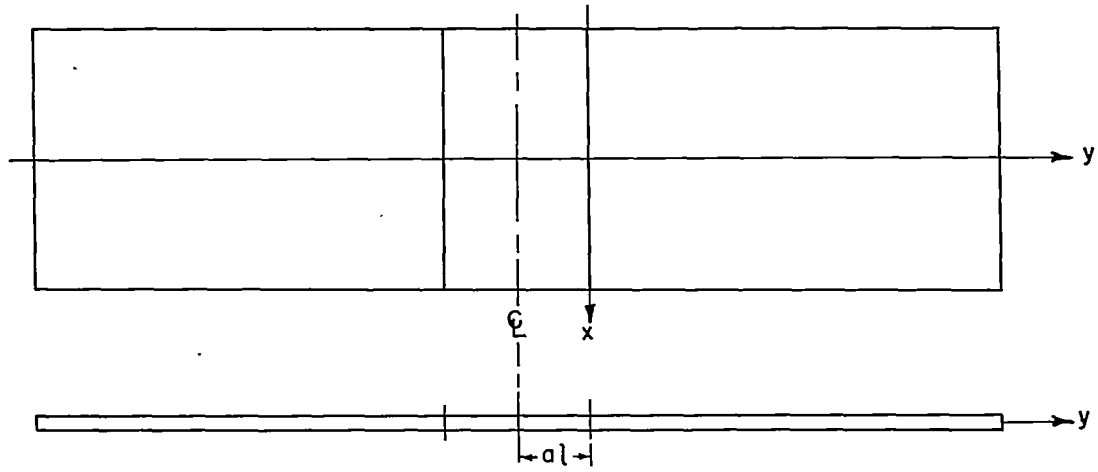

(a) Wing with rigid-plate center section.

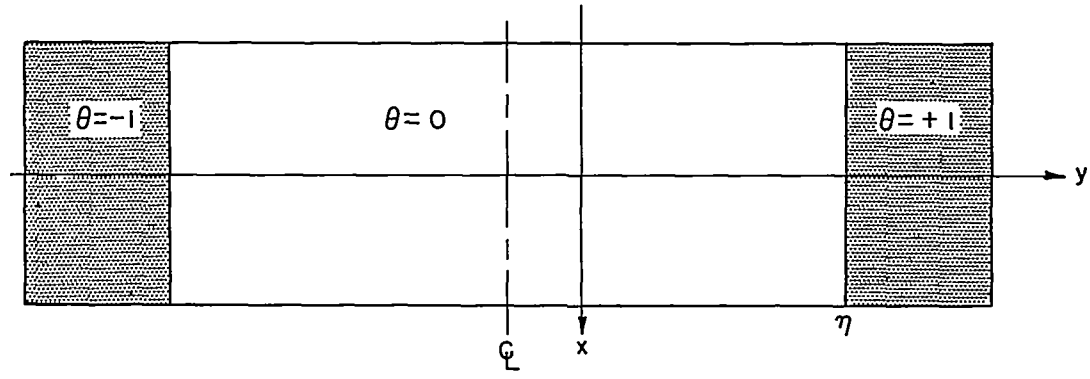

(b) Wing with antisymmetrical unit-step angle-of-attack distribution.

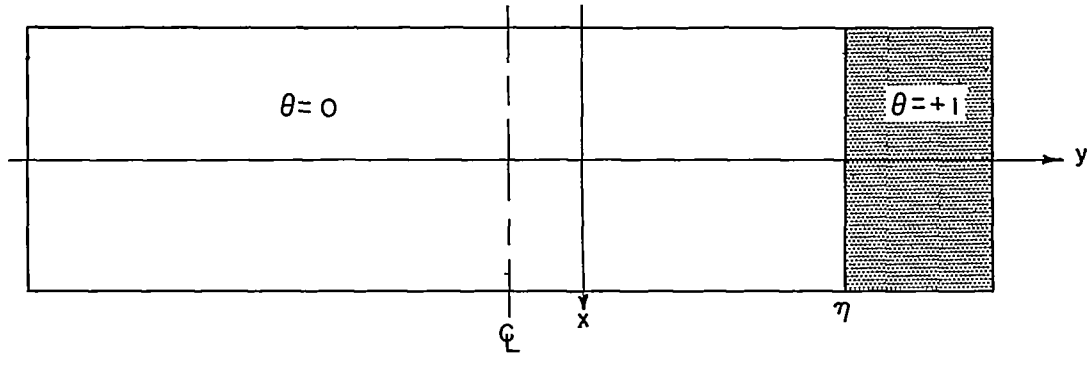

(c) Wing with unit-step angle-of-attack distribution.

Figure 2.- Configurations considered in the aerodynamic analysis.

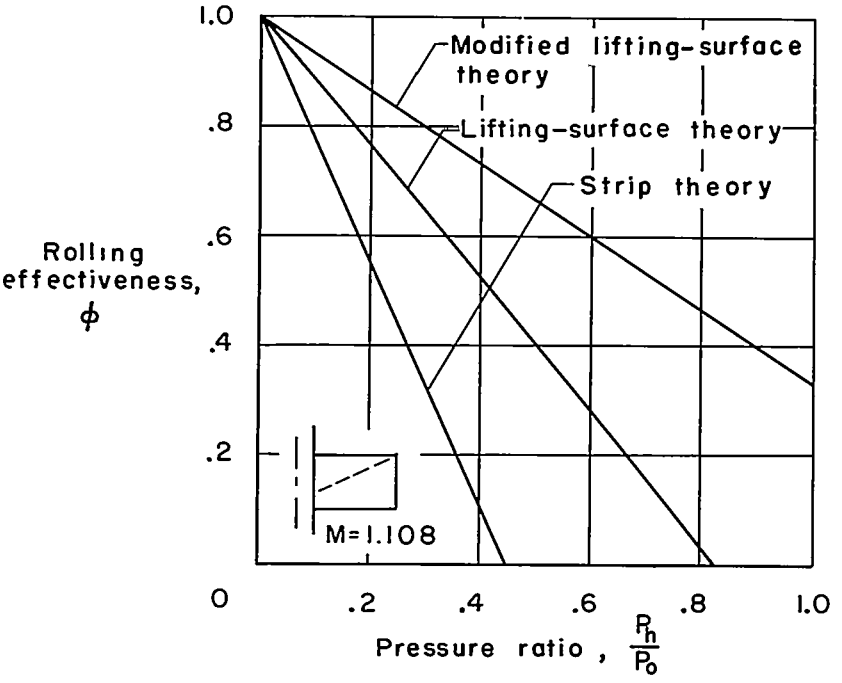

(a) M = 1.108.

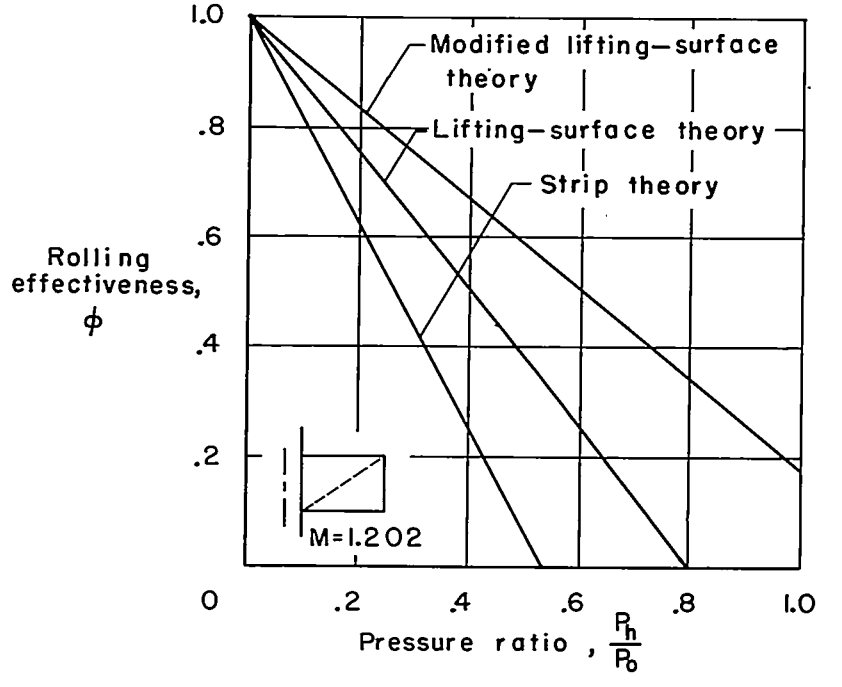

(b) M = 1.202.

Figure 3.- Variation of rolling effectiveness with pressure ratio for constant values of Mach number.

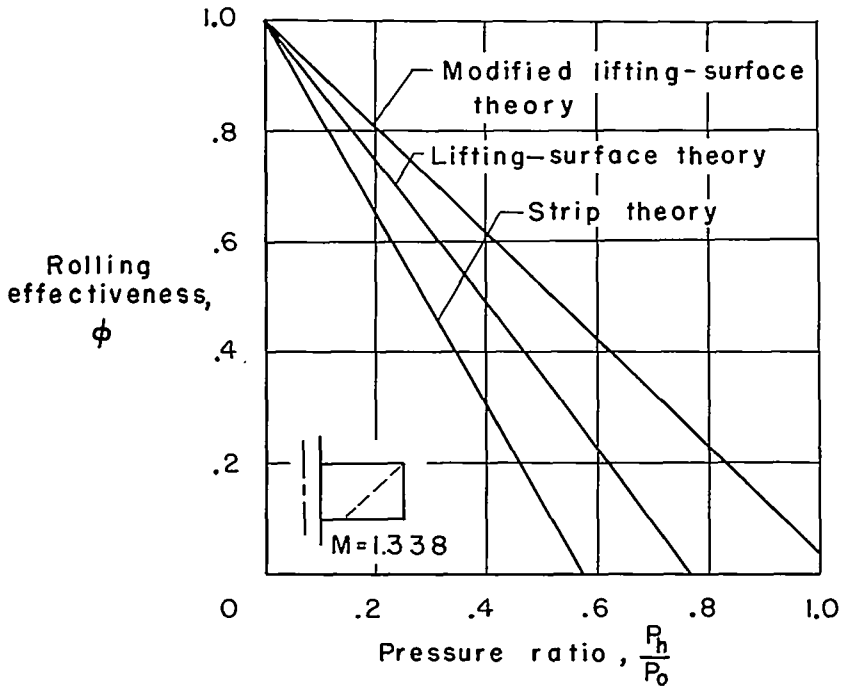

(c) M = 1.338.

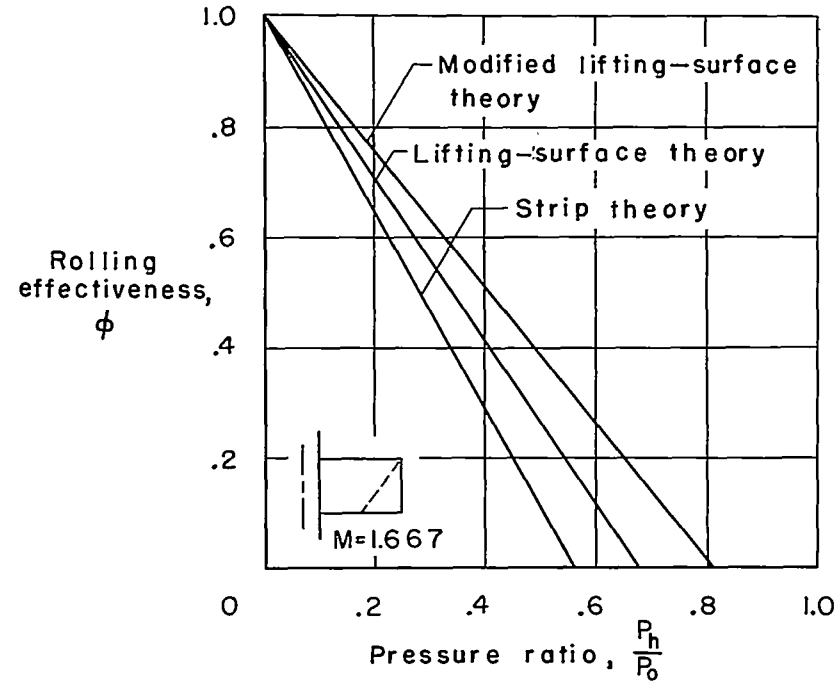

(d) M = 1.667.

Figure 3.- Continued.

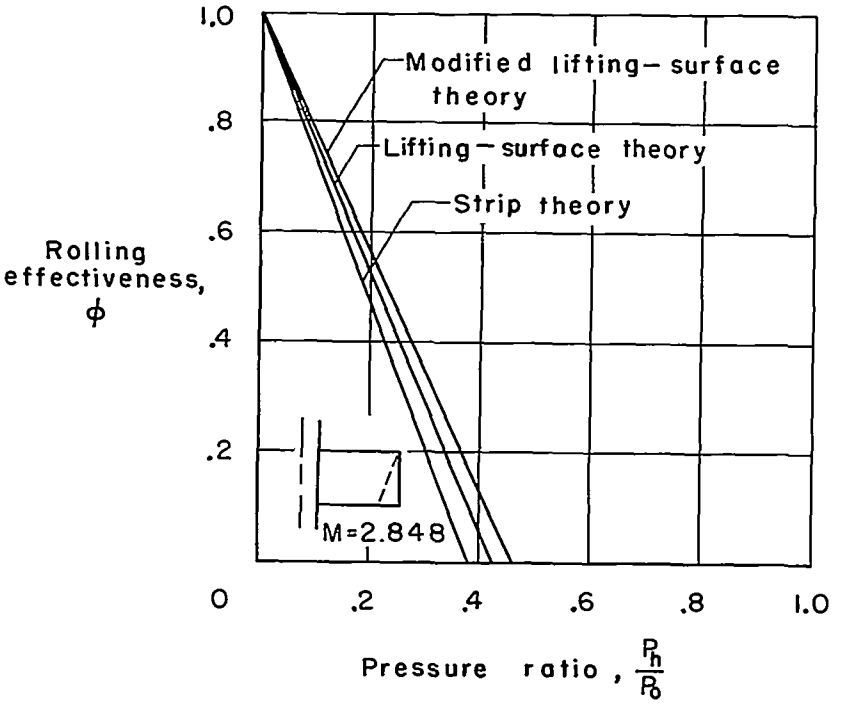

(e) M = 2.848.

Figure 3.- Concluded.

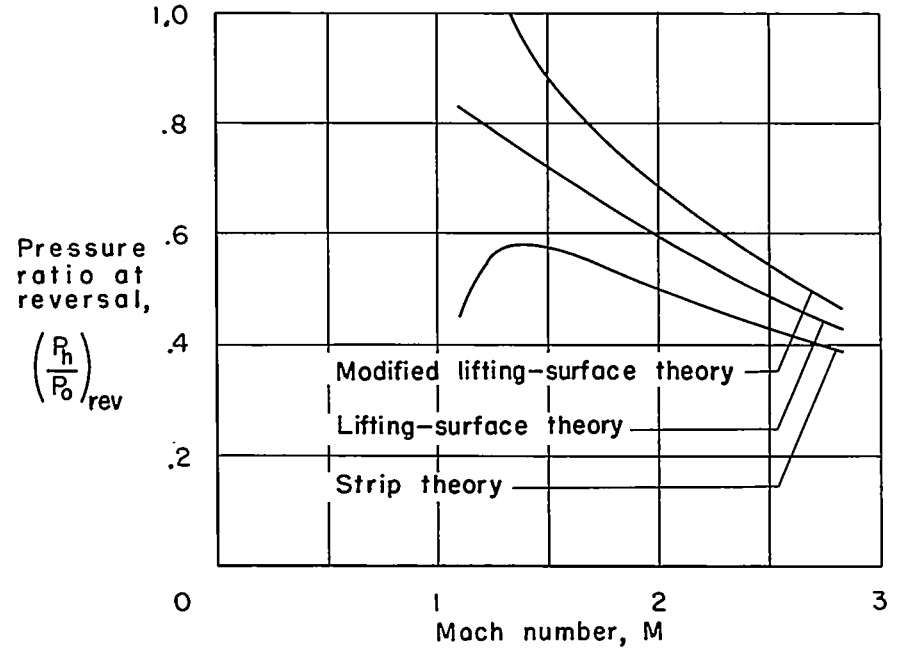

Figure 4.- Variation of pressure ratio at reversal with Mach number.

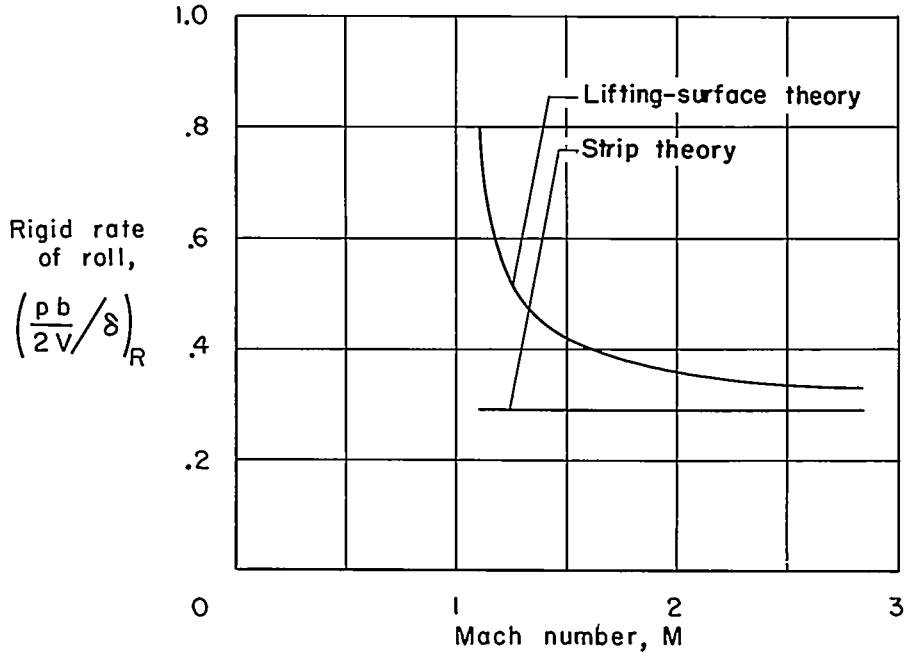

Figure 5.- Variation with Mach number of the rate of roll for the rigid wing.

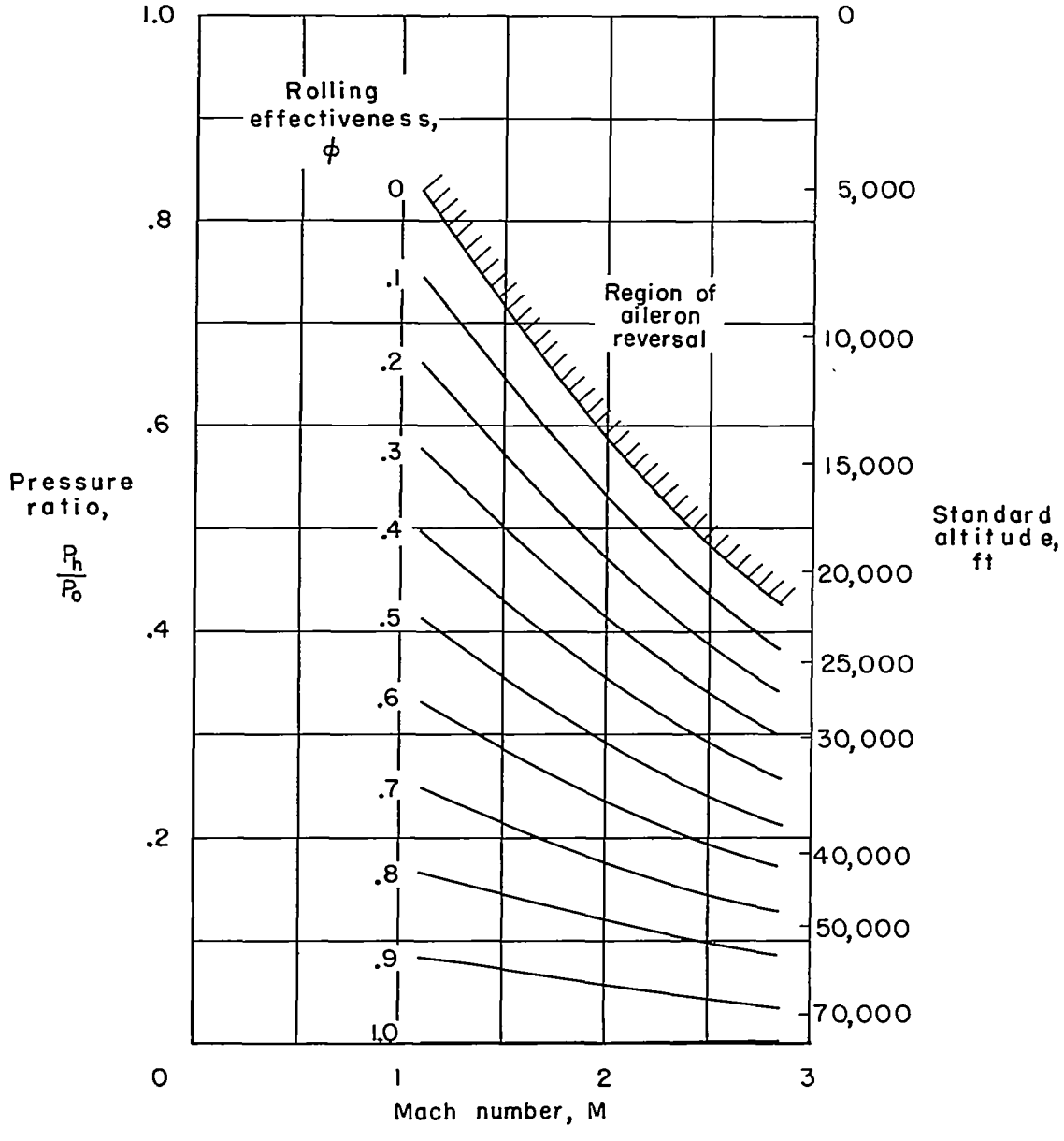

Figure 6.- Variation of pressure ratio with Mach number for constant values of rolling effectiveness.

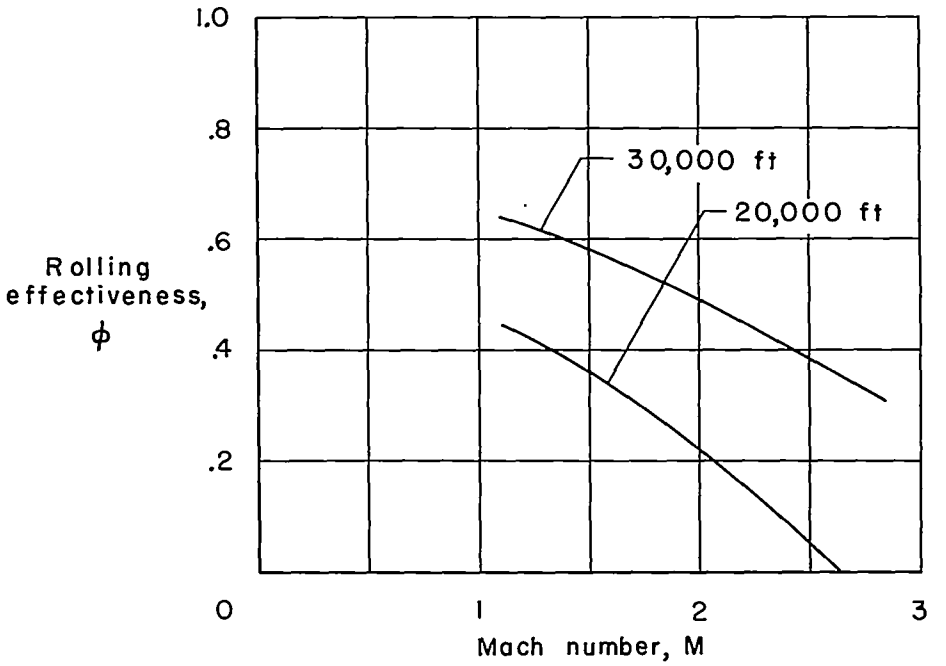

Figure 7.- Variation of rolling effectiveness with Mach number at constant altitude.

NACA-Langley - 4-28-54 - 1000